A MULTI-ORGAN ROLE FOR NOCTURNIN IN POST-TRANSCRIPTIONAL REGULATION OF RNA

APPROVED BY SUPERVISORY COMMITTEE

Carla B. Green, Ph.D., Advisor

Kimberly Huber, Ph.D., Chair, Examining Committee

Joseph Takahashi, Ph.D.

Gang Yu, Ph.D.

Prashant Mishra, Ph.D.

DEDICATION

To my father

A MULTI-ORGAN ROLE FOR NOCTURNIN IN POST-TRANSCRIPTIONAL REGULATION OF RNA

by

YASEMIN ONDER

DISSERTATION / THESIS

Presented to the Faculty of the Graduate School of Biomedical Sciences

The University of Texas Southwestern Medical Center at Dallas

In Partial Fulfillment of the Requirements

For the Degree of

DOCTOR OF PHILOSOPHY

The University of Texas Southwestern Medical Center at Dallas

Dallas, Texas

May, 2018

ACKNOWLEDGEMENTS

I would like to acknowledge my mentor Dr. Carla B. Green, for pushing me to become an independent scientist and for giving me the freedom to explore my research interests throughout my graduate training and for generously providing the resources to enable my scientific pursuits. I would like to thank current and past members of Green lab, Dr. Jeremy Stubblefield, Dr. Clark Rosensweig, Isara Laothamatas, Dr. Peng Gao, Dr. Katharina Sewart for technical help and their feedback on my projects during lab meetings as well as their friendship. I would also like to thank members of Takahashi lab and Drs. Joseph Takahashi and Shin Yamazaki, for their valuable feedback during joint lab meetings.

I am also grateful to the members of my thesis committee, Drs. Kimberly Huber, Joseph Takahashi, Gang Yu, and Prashant Mishra for sharing their expertise and for providing valuable feedback and support during my graduate training. I would like to give special thanks to my thesis committee chair Dr. Kimberly Huber, for her support as a member of my committee as well as for welcoming me in her lab during our collaboration. I would like to acknowledge Huber lab members for making me feel at home during our collaboration and I would like to give special thanks to Dr. Gemma Molinaro for training me on electrophysiology.

Additionally, I would like to give special thanks to members of Mishra lab and Dr. Prashant Mishra for a wonderful collaboration, which was instrumental for my project to grow and to become its final form. Dr. Prashant Mishra, I cannot thank you enough, for sharing your valuable expertise and for the hours you spent on scientific discussions

regarding my project and the priceless feedback you provided. I couldn't have done it without your help.

I would like to express my gratitude for my friends and family for their unfaltering support and encouragement. I would like to give special thanks to Hunkar Gizem Yesilyurt, Didem Agac, Kacey Rajkovich, Flora Farago, Pavlina Todorova, Shino Murakami, Marina Maksimova, Phyllis Lee, Ayse Ece Ercan, JP Saha, Muratcan Cobanoglu, Granny Lambert. I would also like to thank my long-time friends Gokce Ozer and Sila Karakaya, whose support I always feel no matter the distance. Thank you for being there for me through thick and thin. I would like to express my wholehearted thanks to Patrick A. Vizard, for his endless support and encouragement and for being there for me through the most difficult times.

I would like to thank my family for their unconditional love and support. I would like to give special thanks to my mother Sukran Onder, my grandmother Kadriye Ersoy and my aunt Nurhan Vatansever for their endless support.

Finally, none of this would have been possible without the unconditional love and the endless sacrifice of my beloved father, M. Yalcin Onder and this work is dedicated to his memory.

A MULTI-ORGAN ROLE FOR NOCTURNIN IN POST-TRANSCRIPTIONAL REGULATION OF RNA

Publication No._____

Yasemin Onder, M.S.

The University of Texas Southwestern Medical Center at Dallas, 2018

Supervising Professor: Carla B. Green, Professor

Nocturnin is an RNA-specific nuclease, a circadian deadenylase first discovered in the retina of Xenopus laevis, and is conserved among eukaryotes. Nocturnin is widely expressed in the brain and in the periphery and is also an immediate early gene that is acutely induced in response to various stimuli. This study investigates Nocturnin's potential role in post-transcriptional regulation of mRNAs in the mitochondria and in two different tissues: brain and brown adipose tissue (BAT).

Nocturnin has a predicted mitochondrial-localization signal (MLS) surrounded by two potential translation initiation sites (AUG codons) raising the possibility of dual translation initiation sites. Here we demonstrate that Nocturnin is present in the mitochondria

and that it exhibits mitochondrial or cytoplasmic localization via the use of alternative translation initiation sites. I also show that Nocturnin is acutely induced in response to cold and mitochondrially-encoded mRNAs in *Noc-/-* BAT exhibit impaired stability upon cold exposure. Global analysis of cold-induced changes in the transcriptome of *Noc-/-* and wild type (WT) mice reveal down-regulation of glycan biosynthesis genes in the *Noc-/-* BAT. Strikingly, metabolomics analysis demonstrates robust alterations in key tricarboxylic acid metabolites like pyruvate and succinate in the *Noc-/-* mice BAT in response to a prolonged cold exposure. In summary, we propose a model that Nocturnin acts as a metabolic switch in response to cold by diverting glucose and free fatty acids (FFA) to the mitochondria.

In this study, Nocturnin's potential role in post-transcriptional regulation of synaptic plasticity is also investigated. Activity-dependent local protein translation in the dendrites is thought to be an important component of synaptic plasticity. The mechanism of how translation of different mRNAs is differentially regulated in the dendrites is yet not clear. Here I demonstrate that Nocturnin is present in the dendrites as well as in the post-synaptic density as observed in cultured neurons and brain slices from cortex and hippocampus. I investigated mGluR-LTD in hippocampal slices from *Noc-/-* and WT littermates and observed an attenuation of mGluR-LTD in *Noc-/-* mice in the first cohort, but this result was not replicated in a second cohort. Further studies are needed to elucidate Nocturnin's role in the synapse.

TABLE OF CONTENTS

PRIOR PUBLICATIONS

Onder Y, Green CB. Rhythms of metabolism in adipose tissue and mitochondria. *Neurobiology of Sleep and Circadian Rhythms* (in press).

Na ES, De Jesus-Cortes H, Kabir ZD, Wang J, Ramesh V, Onder Y, Rajadhyaksha A, Monteggia LM, and Pieper AA. (2017) D-cycloserine safely improves synaptic transmission in an animal model of Rett syndrome. PLoS ONE 12(8): e018026.

LIST OF FIGURES AND TABLES

LIST OF APPENDICES

CHAPTER ONE

INTRODUCTION

Circadian Rhythms

Many organisms have an intrinsic clock, in order to adapt to the daily changes in the environment resulting from the 24-hour rotations of the Earth. In mammals, the intrinsic circadian system is composed of a central clock in the brain and many peripheral clocks organized in a hierarchical manner. The hypothalamic suprachiasmatic nucleus (SCN) contains the central clock, which is entrained mainly by light input and uses this information to synchronize the peripheral clocks. It should be noted that peripheral clocks can also be entrained via feeding or by humoral cues. At the molecular level, the core clock machinery is comprised of transcription/translation feedback loops, with the core transcription factors CLOCK and BMAL1 activating transcription of *Period* (*Per*) and *Cryptochrome* (*Cry*) genes, the protein products of which form a complex that in turn represses the CLOCK:BMAL1 activity (Green et al., 2008; Partch et al., 2014). Rhythmic *Bmal1* expression is further regulated by nuclear receptors REV-ERB (consisting of REV-ERBα and REV-ERBβ) and retinoic acid receptor-related orphan receptors (RORs; consisting of RORα, RORβ and RORγ), which repress and activate the transcription of *Bmal1,* respectively.

According to early microarray studies from mouse SCN, liver and heart tissues, around 10% of the transcriptome is rhythmic (Akhtar et al., 2002; Panda et al., 2002; Storch et al., 2002; Ueda et al., 2002). A more recent global transcriptome study utilizing RNA-seq and DNA arrays on 12 mouse organs revealed that 43% of all protein coding genes were cycling at least in one organ (Zhang et al., 2014). Cycling of genes was observed in all 12 organs in a tissue specific manner, within a range of 3-16 %. Liver had the largest amount of cycling genes with 16% and hypothalamus had the lowest with 3%. Aside from the core clock genes, these rhythmic genes are CLOCK-regulated circadian output genes that are either direct targets of CLOCK/BMAL via an E box element in their promoter region or indirect targets via CLOCK interaction with transcription factors (Grechez-Cassiau et al., 2004; Miller et al., 2007; Oishi et al., 2003; Panda et al., 2002). Notably, these output genes are involved in key physiological functions like transcription, metabolism, cell proliferation and immune function as well as many other downstream signaling pathways. Interestingly, when the rhythmic transcriptome is compared to the rhythmic proteome, there is a mismatch between the percent of oscillating transcripts and oscillating proteins from mouse liver, with almost 2-fold more oscillating proteins than transcripts (Mauvoisin et al., 2014; Reddy et al., 2006; Robles et al., 2014). This suggests post-transcriptional or post-translational mechanisms are in play in regulating the circadian rhythmicity. Moreover, ribosome profiling studies from U2OS cells and mouse liver revealed rhythmic changes in ribosome occupancy and found ribosome profiling data as a better predictor of rhythmicity than transcription itself, indicating an important role for circadian regulation of translation (Jang et al., 2015; Janich et al., 2015). Lastly, the analysis of pre-mRNA or nascent RNA levels revealed that

many cycling mRNAs do not exhibit corresponding oscillations in nascent RNA level, suggesting major contribution to circadian transcriptome by post-transcriptional mechanisms (Koike et al., 2012; Kojima et al., 2012; Lim and Allada, 2013; Menet et al., 2012).

Polyadenylation and Deadenylation as Post-Transcriptional Mechanisms

Polyadenylation and deadenylation are post-transcriptional mechanisms that act on mRNA stability. The addition of the poly(A) tail at the 3' end of the mRNA transcript is the final step of mRNA processing and is thought to increase transcript stability (Weill et al., 2012; Zhang et al., 2010). One of the early reports of rhythmic polyadenylation was of vasopressin mRNA in the SCN (Robinson et al., 1988). In concordance with the contribution of post-transcriptional mechanisms in circadian rhythms, 2-3% of the expressed mRNAs in mouse liver were found to have diurnal rhythms in polyadenylation that is closely correlated to rhythmic protein expression. Importantly, 20% of these genes did not have corresponding steady state mRNA rhythmicity (Kojima et al., 2012). Moreover, some of the common genes encoding components of the polyadenylation/deadenylation machinery like *Parn*, *Cbep* and *Gld2* were rhythmically expressed in phase with the poly(A) rhythms.

Deadenylation, on the other hand, is the cleavage of the poly(A) tail which leads to silencing or degradation of mRNAs. Two main families of known deadenylases are DEDD and exonuclease-endonuclease-phosphatase (EED) families (Goldstrohm and Wickens, 2008). Some major deadenylases in the DEDD family are CAF1, PARN and PAN2 and deadenylases that belong to EEP family are CCR4, Nocturnin, ANGEL, 2'phoshodiesterase

(2'PDE). CAF1, PAN2, CCR4, Nocturnin and ANGEL are widely conserved in eukaryotes, whereas PARN is conserved in vertebrates. In experiments measuring mRNA decay kinetics in NIH3T3 fibroblasts, PAN2 and CCR4 were identified as major poly(A) nucleases leading cytoplasmic deadenylation and nonsense-mediated decay (Yamashita et al., 2005). Another well characterized deadenylase that is conserved in a wide range of organisms from plants to vertebrates is PARN [reviewed in (Godwin et al., 2013)], which was found to have rhythmic transcript levels in mouse liver (Kojima et al., 2012). These different deadenylases were found to effect a multitude of biological functions in the organisms, ranging from homeostasis to DNA damage, suggesting that this variety in deadenylases with possible different targets could facilitate a diverse multifunctional control of mRNA.

Nocturnin

Nocturnin (*Noct*, *Ccrn4l*) was first discovered in a differential display screen for the rhythmic genes in the *Xenopus laevis* retina (Green and Besharse, 1996). Upon investigation of Nocturnin's function, it was uncovered that Nocturnin is a deadenylase, belonging to CCR4 family based on sequence homology (Baggs and Green, 2003). Thus, it shares a common core catalytic domain at its C-terminus with the other CCR4 family members, but shows distinction in its N-terminus. *Nocturnin* is widely conserved among eukaryotes and is expressed ubiquitously in many organs and tissues in mammals (Wang et al., 2001). Notably, *Nocturnin* is rhythmic in many of these tissues including liver, muscle, kidney and intestine with its expression peaking at early night.

Nocturnin is an output gene of the core circadian clock machinery (Oishi et al., 2003) and is regulated directly by the CLOCK/BMAL binding to the E box element in its promoter region (Li et al., 2008) as well as by other rhythmic signals. It is not part of the core clock machinery as *Noc-/-* mice have no behavioral circadian deficits and they sustain the rhythmicity of their core clock genes (Green et al., 2007). Additionally, Nocturnin has also been identified as an immediate early gene, and it is acutely induced in response to a number of stimuli like serum shock, lipopolysaccharide (LPS), and peroxisome proliferator-activated receptorγ (PPARγ) agonist rosiglitazone (Garbarino-Pico et al., 2007; Kawai et al., 2010b; Niu et al., 2011). Nocturnin can also be induced by nutrient and metabolic cues like high-fat diet and olive oil gavage (Douris et al., 2011; Green et al., 2007; Stubblefield et al., 2018) . Not surprisingly, Nocturnin is implicated in a wide range of physiological functions like lipid metabolism (Green et al., 2007; Stubblefield et al., 2018), adipogenesis (Kawai et al., 2010b), osteogenesis (Kawai et al., 2010a) and immune function (Niu et al., 2011). Nocturnin's deadenylase function combined with its capacity to respond to metabolic/environmental cues makes it a likely candidate for fine-tuning the responses towards organismal and environmental demands through post-transcriptional regulation across a number of tissues.

This thesis further investigates Nocturnin's potential role in the post-transcriptional regulation of brown fat thermogenesis and mitochondrial function (Chapter 2) and synaptic plasticity (Chapter 3).

CHAPTER TWO

MODULATION OF BROWN FAT THERMOGENESIS AND MITOCHONDRIAL FUNCTION BY THE CIRCADIAN DEADENYLASE NOCTURNIN

Introduction*

The prevalence of metabolic disorders like obesity has been rising at alarming rates over the last several decades. According to a 2010 report (Hammond and Levine, 2010), more than two-thirds of the American population are overweight. In addition, obesity is also closely linked to many other diseases, such as hypertension, type 2 diabetes, coronary heart disease, stroke and several types of cancer, significantly adding to the economic cost of this epidemic to society (Hammond and Levine, 2010). Obesity is related to abnormalities in adipose tissue and mitochondrial dysfunction: normal energy metabolism requires an intricate balance of energy storage and energy dissipation via adipose tissue and mitochondrial function and in obesity this balance is tipped to favor triglyceride (TG) storage over lipid oxidation (Bjorndal et al., 2011).

*Parts of this chapter were published in Onder Y, Green CB. Rhythms of metabolism in adipose tissue and mitochondria. *Neurobiology of Sleep and Circadian Rhythms* (in press).

The Role of Adipose Tissue and Mitochondria

Adipose tissue is a dynamic endocrine organ, central to whole-body energy homeostasis. In mammals, there are three types of adipose tissue: White adipose tissue (WAT), brown adipose tissue (BAT), and beige or brite adipose tissue (iBAT). WAT is involved in energy storage whereas BAT is responsible for energy dissipation in the form of heat through non-shivering thermogenesis. In addition to their opposite functions, BAT and WAT are also structurally quite different. WAT cells are spherical in shape and are composed of a single large lipid droplet along with a small number of mitochondria, whereas BAT cells are small and ellipsoid with multiple small lipid droplets and a large number of mitochondria (Cedikova et al., 2016; Harms and Seale, 2013). Beige adipocytes, on the other hand, have a mix of BAT and WAT characteristics both structurally and functionally, as they have more WAT-like properties at basal state, but they can acquire BAT-like thermogenic features upon activation of sympathetic nervous system by a stimulus like cold. Cold exposure is the predominant activator of BAT and the beiging of WAT in mammals, although it should be noted that in recent years exercise and irisin were also shown to activate these mechanisms (Virtanen, 2014). WAT is mainly located subcutaneously and viscerally and BAT is located in interscapular, cervical, axillary and perirenal space in mice. Human BAT is comprised of a mix of classical brown and beige adipocytes and these depots are in the cervical, supraclavicular, suprarenal and paravertebral regions.

Mitochondria have a vital role in energy metabolism and are essential for sustaining proper functioning of the complementary energy storage and energy dissipation functions that occur in the WAT and the BAT, respectively. Mitochondria are involved in lipolysis

and lipogenesis, which are the major functions of WAT. In lipolysis, triglycerides are hydrolyzed from lipid droplets into glycerol and free fatty acids (FFA). These FFAs are then transferred into the mitochondria, either by diffusion or by carnitine shuttle for long-chain fatty acids. Consecutively, fatty acids are broken down into acetyl-CoA by β-oxidation in the mitochondrial matrix. Finally, acetyl-CoA is oxidized through the tricarboxylic acid cycle (TCA) and ATP is generated through oxidative phosphorylation by the electron transport chain (ETC). On the other hand, lipogenesis is the conversion of fatty acids to triglycerides for storage in the WAT as lipid droplets. Although lipogenesis occurs in the cytosol, the two important intermediates for lipogenesis; glycerol 3-phosphate and acetyl-CoA are generated in the mitochondria (Cedikova et al., 2016).

On the other end of the energetics spectrum, BAT mitochondria are essential for non-shivering thermogenesis. These specialized mitochondria have uncoupling protein 1 (UCP1) transported to their inner mitochondrial membrane, when activated by cold or by β-adrenergic (β-AR) stimulation. Upon stimulation, UCP1 uncouples the mitochondria by increasing the membrane conductance and dissipates the proton gradient required for ATP synthase function. This results in the energy of oxidized substrates being converted into heat rather than being used in ATP production. This whole process is called thermogenesis (Fedorenko et al., 2012).

In cases of metabolic imbalance as in obesity, excessive nutrient supply leads to high levels of glucose and FFAs in WAT and to accommodate this surplus, WAT expands and remodels itself. These adaptive responses include reduced mitochondrial number and function, reduced mitochondrial biogenesis, reduced OXPHOS and ATP production and

increased amounts of ROS production, which results in dysfunctional hypertropic adipocytes. BAT activity on the other hand is thought to be counter-obesity, as increased BAT activity is linked to obesity-resistance in many mouse models. Additionally, in obese humans, lower mass and activity of UCP1-expressing adipocytes has been reported (reviewed in (Cedikova et al., 2016).

Circadian Regulation of Adipose Tissue and Mitochondria

The circadian clock is an important mediator of metabolism, which is also closely related to metabolic disorders like obesity (Brum et al., 2015; Karlsson, 2001; Lamia et al., 2008; Marcheva et al., 2010; Mukherji et al., 2015; Oishi et al., 2006; Rudic et al., 2004; Turek et al., 2005). The regulation of energy homeostasis and metabolic function requires the orchestrated action of the hypothalamic suprachiasmatic nucleus (SCN) and the peripheral clocks. Adipose tissue is a key component of energy metabolism, and growing evidence supports its control by the circadian clock. Rhythmic expression of circadian clock genes have been characterized in adipose tissues by microarray and RNA-sequencing studies (Zhang et al., 2014; Zvonic et al., 2006). According to the murine circadian gene expression atlas, 8% of the protein-coding genes in BAT and 4% of the genes in WAT are rhythmic (Zhang et al., 2014). Some important functions of the adipose tissue, lipolysis and the release of free fatty acids (FFAs) and glycerol have also been reported to have diurnal rhythms (Shostak et al., 2013). These rhythms were altered in *Clock* mutant mice, along with decreased lipolysis, increased adiposity and increased sensitivity to fasting (Shostak et al.,

2013). Interestingly, these animals were not able to maintain their body temperature following 12 hours of fasting, which could indicate impaired BAT thermogenesis. In order to identify the contribution of the adipocyte clocks per se in forming these metabolic phenotypes, conditional knockout mice that had an adipocyte-specific deletion of Bmal1 were used(Paschos et al., 2012). These mice developed obesity along with having reduced energy expenditure and altered food intake rhythms. They also had reduced polyunsaturated fatty acids in adipose tissue, plasma and hypothalamus. This FFA reduction in hypothalamus was inversely correlated with an increase in hypothalamic neuropeptides that regulate feeding activity, and was reversed by a polyunsaturated fatty-acid rich diet. This finding is interesting since it suggests bidirectional communication between hypothalamic feeding centers and adipocyte clocks. Thus, the adipocyte clock regulates the rhythmic fatty acid release into the circulation which in turn entrains the rhythmic feeding behavior. These studies are important in showing the importance of adipocyte clocks in metabolism, and how feedback from the peripheral clocks to the hypothalamus is required for maintaining energy homeostasis.

Circadian Regulation of Brown Adipose Tissue and Thermogenesis

BAT is a specialized fat tissue, which is enriched in mitochondria and oxidative capacity and is known for its thermogenic properties. The discovery of brown fat is relatively new; its thermogenic properties were not known until the 1960s (Cannon and Nedergaard, 2004). More recently it became an exciting area of research, as its potential anti-obesity

properties have been revealed (Feldmann et al., 2009; Kontani et al., 2005; Lowell et al., 1993; Saito et al., 2009). In mammals, upon cold exposure or food intake noradrenergic circuits are activated, which in turn activate BAT via UCP-1, which uncouples the mitochondria and converts FFAs into heat.

In addition to the activation of BAT by cold exposure, research suggests a concerted action between the SCN, ventromedial hypothalamus and the BAT clock, in order to achieve energy homeostasis fine-tuned to adapt to the daily environmental demands. Recent studies provided some mechanistic insight into the circadian regulation of brown fat thermogenesis. Core clock genes were induced upon cold-exposure in the BAT but not in the WAT, and this process is mediated by the β-adrenergic signaling and PGC1-α (Li et al., 2013). Paradoxically, *Bmal1* knockout mice did not have a defect in thermogenesis, despite having altered expression of genes involved in lipid metabolism and adaptive thermogenesis. A possible explanation for this contradictory finding could be that the circadian nuclear receptor REV-ERBα is a direct repressor of *Ucp1* (Gerhart-Hines et al., 2013). Wild type mice had reduced cold tolerance at ZT4-10, which is the peak of *Rev-erbα* (gene name *Nr1d1*) mRNA expression and this diurnal variation in cold sensitivity was abolished in the *Rev-erbα* -/- mice. Further, they showed that cold exposure rapidly down-regulates *Rev-erbα*, in parallel with an induction of *Ucp1*, and independent of noradrenergic stimulation. This study was important to establish how a circadian transcriptional repressor, REV-ERBα, integrates the circadian oscillators with the environmental demands in the BAT. This circadian regulation of *Ucp1* and thermogenesis could be serving the organism as an energy

saving mechanism, where thermogenesis is repressed during sleep when mammals are not active.

The sleep/wake and fasting/feeding cycles are essential in the link between the circadian clock and metabolism. Disturbances in the time of feeding and shift work have metabolic consequences, as previously mentioned. The master clock in the SCN is mainly entrained by the light input whereas many peripheral clocks could be entrained by food intake (Green et al., 2008). How BAT is effected by this entrainment of the circadian clock by food and light input has been investigated. One study showed that food entrained phase shifts of the circadian genes were significantly prolonged in the BAT from mice lacking the alpha isoform of perixosome proliferators-activated receptors *(Ppara-/-* mice*)* compared to wild-type mice (Goh et al., 2007), supporting a role for a food-entrainable circadian transcriptional regulator in BAT. Another study investigated the effects of time-restricted feeding of a high fat diet (HFD) on metabolic diseases (Hatori et al., 2012). One interesting finding from this study was that, compared to the ad lib HFD group, mice that were fed HFD time-restricted to their natural nocturnal feeding period had increased thermogenesis, improved nutrient utilization and reduced adiposity. Additionally, they had enhanced rhythmicity of the thermogenic genes and improved BAT morphology. A recent study by Orozco-Solis and colleagues provided mechanistic insight into how these environmental zeitgebers are integrated to circadian energetics in BAT (Orozco-Solis et al., 2016). Ventromedial hypothalamus (VMH) is thought to be involved in the regulation of food intake and metabolism. This study used a conditional knockout mouse model, that is lacking *Bmal1* specifically in the steroidogenic factor1 (SF1) neurons in the VMH, which are known to

regulate diet-induced thermogenesis (Orozco-Solis et al., 2016). Disruption of the VMH clock in these mice resulted in increased energy expenditure and thermogenic capacity, despite having intact SCN and endogenous BAT clocks. These findings suggest that the VMH clock collects input from the environmental zeitgebers to modulate cyclic thermogenesis via adrenergic receptors, independent of the SCN and the endogenous BAT clock. Together with the previous studies, bidirectional communication between the adipocyte-hypothalamic axis clocks seems to be important to coordinate energy expenditure and feeding rhythms. These findings could also point to interesting therapeutic possibilities like time-restricted feeding or cold exposure as a means of facilitating thermogenic pathways.

The existence of brown adipose tissue in humans was not confirmed until the last decade (Cypess et al., 2009; van Marken Lichtenbelt et al., 2009; Virtanen et al., 2009). This relatively new finding created a lot of interest due to the potential therapeutic use of BAT activation in metabolic diseases. Activation of human brown fat via cold or β-adrenergic agonists has been shown to increase BAT metabolic activity and the resting metabolic rate (Cypess et al., 2015). A diurnal rhythm in glucose uptake in BAT has previously been shown in rodents in vivo with PET imaging (van der Veen et al., 2012). In a recent study, in vivo, in vitro and ex vivo experiments with human BAT showed consistencies with rodent data (Lee et al., 2016). The study revealed a thermogenic circadian rhythm in human BAT, that is glucose responsive. It has also demonstrated circadian rhythmicity of *Ucp1*, *Glut4* and *Rev-erbα*, in both differentiated human brown adipocytes and human BAT explants. The glucose rhythms in patients showed greater fluctuations in patients with less BAT abundance, which

might suggest that BAT acts as a buffer for glycemia. Although more studies to confirm this correlation are needed, this potential glucose-modulatory role of BAT in humans could lead to new therapeutic approaches in treating hyperglycemia and diabetes.

Circadian Control of Oxidation and Nutrient Utilization

Mitochondria are critical hubs for energy metabolism and homeostasis in eukaryotic cells. Originally evolved from a prokaryotic ancestor, mitochondria produce more than 95% of the ATP that is required for the cellular processes (Cedikova et al., 2016). In addition to its main function, which is synthesizing ATP through oxidative phosphorylation, mitochondria also contribute to energy homeostasis in many other ways, including facilitation of lipolysis through fatty acid oxidation, contributing to maintenance of Ca^{2+} homeostasis, and regulation of apoptosis via reactive oxygen species (ROS) production (Cedikova et al., 2016; Vakifahmetoglu-Norberg et al., 2017). Considering the dynamic nature of mitochondria, which adapt to the metabolic needs of the cell, it is not surprising that a strong link between the circadian clock and the mitochondrial function exists.

Rhythmic food intake is one of the central clock outputs and is known to have a profound effect on metabolism. Nutrient status is critical in determining the temporal regulation of mitochondrial function as it provides the oxidizable substrates for the electron transport chain and oxidative phosphorylation. It was unclear, though, if the oxidation of these substrates in the mitochondria has self-sustained rhythms. Previously it has been reported that nicotinamide phosphoribosyltransferase (NAMPT), the rate limiting enzyme for

NAD^+ biosynthesis, is under direct control of the circadian clock, which results in rhythmic NAD^+ levels (Nakahata et al., 2009). More recently, Peek and colleagues found that these rhythmic NAD^+ levels are coupled by rhythms in fatty acid oxidation and mitochondrial respiration. Most importantly, they showed that these NAD^+-dependent rhythms are self-sustained (Peek CB, 2013). Thus, the rhythms persisted even under constant nutrient status. Supporting that these rhythms are governed by the circadian clock, the study reported reduced mitochondrial NAD^+ and fatty acid oxidation levels in livers from fasted *Bmal1* -/- mice. Proteomics on isolated mouse liver mitochondria from another study revealed that 38% of the mitochondrial proteins oscillate diurnally, providing additional evidence to the circadian control of mitochondrial function (Neufeld-Cohen et al., 2016). Notably, a number of rate-limiting enzymes that are critical for mitochondrial metabolic pathways showed diurnal oscillations. One of those rhythmic enzymes was carnitine palmitoyltransferase-1 (CPT1), which is critical for the transport of long-chain fatty acids through the carnitine shuttle for fatty acid oxidation. Collectively, these studies reveal circadian control of nutrient utilization and mitochondrial oxidative metabolism. The self-sustained metabolic rhythms are a possible adaptation to the daily activity and rest cycles as they let the organism be most efficient energetically by making metabolic activity peak just before the period that mice are most active.

Rhythmic Post-Translational and Post-Transcriptional Modifications in the Mitochondria

Circadian rhythms in the absence of transcription have been reported in a eukaryote (O'Neill et al., 2011; Woolum, 1991), which might point to post-translational mechanisms in the regulation of the circadian clock. In support of this, there is a mismatch between the percent of oscillating transcripts and oscillating proteins from mouse liver, with almost 2-fold more oscillating proteins than transcripts (Mauvoisin et al., 2014; Reddy et al., 2006; Robles et al., 2014). Interestingly, there is also a discrepancy between the cycling mitochondrial proteome and transcriptome (Neufeld-Cohen et al., 2016). A number of studies reported circadian regulation of mitochondria via rhythmic acetylation. One mass spectrometry based study analyzed genome-wide lysine acetylation in wild type and *Clock-/-* mice livers and revealed clock-driven acetylation in a number of mitochondrial proteins that are involved in metabolic pathways (Masri S, 2013). Regulation of fatty acid oxidation by NAD^+-dependent deacetylase SIRT3 has previously been shown (Hirschey et al., 2010). Circadian control of this process has been revealed by Peek and colleagues, where they showed *Bmal1*-dependent deacetylation of mitochondrial proteins via SIRT3 (Peek CB, 2013). Additionally, a more recent study showed rhythmic complex I activity along with rhythmic acetylation of complex I (Cela et al., 2016). These studies suggest a role for post-translational modifications in circadian time-keeping, particularly in the mitochondria.

Mitochondrial Transcription

Mitochondrial oxidative phosphorylation is achieved by five respiratory chain complexes, that is assembled via the concerted action of 13 mitochondrial-encoded mRNAs (mtRNAs) and around 80 nuclear-encoded proteins that gets transported into the mitochondria (Chinnery, 2015). Mammalian mitochondrial transcription has unique properties as the mitochondria has its own circular genome that is evolved from prokaryotic ancestors. Mitochondrial transcription occurs in a polycistronic manner by the complementary H and L strands of the circular DNA leading to single precursor RNAs that then gets cleaved into mRNAs, rRNAs and tRNAs by endonucleases. This mechanism should lead to equal amounts of RNA species, however, the final steady state RNA levels differ significantly which suggest an important role for post-transcriptional mechanisms in the mitochondrial RNA processing (Rorbach and Minczuk, 2012).

Polyadenylation and Deadenylation in the Mitochondria

How polyadenylation and deadenylation functions in the mitochondria is unclear, as there are conflicting reports in the literature. Early reports investigated if there is a correlation between poly(A) tail length and mitochondrial RNA stability in human cell lines by knocking down mitochondrial poly(A) polymerase (mtPAP). Half of these studies reported decreased steady-state levels of mitochondrial mRNAs *MT-CO1*, *MT-CO2*, *MT-CO3* and *MT-ATP8/6* (but not *MT-ND3*) as a result suggesting mRNA stabilization by

polyadenylation (Nagaike et al., 2005; Nagao et al., 2008). In contrast, other studies reported that the shortening of poly(A) tails of *MT-ND3*, *MT-CO3* and *MT-ATP6/8* transcripts had no effect on transcript stability (Piechota et al., 2006; Tomecki et al., 2004). Another strategy to investigate the link between deadenylation and mitochondrial mRNA stability has been mitochondrial targeting of the deadenylase PARN (Wydro et al., 2010). Upon deadenylation of the transcripts by PARN, steady-state levels of half of the mitochondrial transcripts (*MT-CO1*, *MT-CO2*, *MT-ATP6/8*) were decreased, while transcript levels of the other half (*MT-ND1*, *MT-ND2*, *MT-ND5*) were increased. Later studies identified PDE12 as the first mitochondrial deadenylase and PDE12 overexpression in cultured human cells resulted in a similar bidirectional effect on steady state MT-RNA levels (Rorbach et al., 2011). Notably, the changes in poly(A) tail dynamics were accompanied by inhibition of mitochondrial translation and impaired mitochondrial respiration. Interestingly, a recent study using mitochondrial ribosomal profiling and mitochondrial poly(A)-tail RNA sequencing in PDE12 lacking human cells, reported neither mRNA poly(A) tail length nor mRNA stability was altered (Pearce et al., 2017). However, they observed aberrant adenylation of non-coding mt-tRNAs which resulted in stalling of mitochondrial translation machinery and impaired mitochondrial respiration. This is consistent with another report from *Drosophila melanogaster* that suggested polyadenylation in the mitochondria is not required for translation but rather is important for the maturation of specific mt-tRNAs (Bratic et al., 2016). This study reported mitochondrial translation was intact despite mitochondrial RNAs having incomplete 3' ends without polyadenylation. However, these translated peptides were not functional and OXPHOS machinery was impaired as a result. In combination, these

studies suggest that polyadenylation and deadenylation in the mitochondria are essential for the proper mitochondrial function but the exact mechanism of how they might impact post-transcriptional regulation and translation is rather complex.

Nocturnin's role in metabolism and adipogenesis/osteoblastogenesis

Nocturnin knockout mice have a striking metabolic phenotype, where they remain lean on a high-fat diet and do not develop fatty livers (Green et al., 2007). This lean phenotype could not be explained by hyperactivity or lower caloric intake as *Noc-/-* and WT mice have comparable levels of food intake and activity. Although the initial study reported no differences in the metabolic rate between genotypes, a recent study found higher metabolic rate in *Noc-/-* mice under high-fat diet condition, which could contribute to the lean phenotype (Stubblefield et al., 2018). *Noc-/-* mice also had an increase in triglycerides and non-esterified fatty acids (NEFA) in their circulation upon refeeding (Stubblefield et al., 2018), and had reduced lipid absorption that leads to accumulation of lipid droplets in the intestinal enterocytes which could partially explain the lean phenotype (Douris et al., 2011). At the gene expression level, *Noc-/-* mice had reduced expression of some lipogenic genes in the liver (Green et al., 2007). Interestingly, one recent study reported an increase at peak amplitudes of mRNAs encoding cholesterol and lipid synthesis enzymes in *Noc-/-* mice livers at ZT18, at the time point that Nocturnin levels are supposed to be the highest (Stubblefield et al., 2018). Moreover, there was a corresponding increase at the triglyceride levels at ZT18 in the *Noc-/-* mice. Some of these genes have lengthened Poly(A) tails which might suggest

they are potential Nocturnin targets however we cannot rule out the possibility that these genes might be upregulated in order to compensate for the increase in systemic triglyceride levels.

Interestingly, perixosome proliferator-activated receptor-gamma (*Pparg*), a transcription factor that targets many lipid metabolism genes, loses its circadian rhythmicity in the *Noc-/-* mice (Green et al., 2007). Intriguingly, later studies uncovered that Nocturnin has a role in promoting adipogenesis over osteoblastogenesis via its interaction with PPARγ (Kawai et al., 2010a; Kawai et al., 2010b). Two isoforms of PPARγ have been identified in humans and mice, PPARγ1 which is ubiquitously expressed across tissues and PPARγ2 which is predominant in the adipose tissue. Thus, *Nocturnin* is acutely induced nearly 30-fold in *Pparg2* transfected bone-marrow stromal cells when exposed to Pparg2 agonist rosiglitazone which suggests Nocturnin could be a downstream target of PPARγ. Moreover, Nocturnin physically interacts with PPARγ and stimulates its nuclear translocation and this seems to be independent of Nocturnin's deadenylase function (Kawai et al., 2010b). This finding is interesting as it suggests Nocturnin might have other functions than its presumed function as a deadenylase and it may be forming a feedback loop by activating PPARγ.

The only confirmed Nocturnin target to date is insulin-like growth factor-1(Igf-1) which is a hormone secreted by the liver with crucial functions for growth and development (Kawai et al., 2010a). IGF-1 is also critical for the maintenance of skeletal bone mass. *Noc-/-* mice have been previously reported to have an increase in bone mass with decreased bone marrow adiposity and Nocturnin has been implicated in suppressing osteogenesis (Kawai et al., 2010b). Interestingly, *Igf1*is rhythmic in the femur bone from mice and this rhythm is in

antiphase of Nocturnin. Closer inspection revealed Nocturnin specifically interacts with *Igf1* transcripts with a longer 3'UTR, but not with the forms bearing the shorter 3'UTR and suppresses *Igf1* expression in an osteoblastic cell line (Kawai et al., 2010a). Suppression of *Igf1* expression can be stimulated by Pparg agonist rosiglitazone, with a concomitant increase in *Nocturnin* expression, which suggests Nocturnin could be the intermediary between Pparg and Igf1. Nocturnin's effect on *Igf1* is also tissue-specific as it not observed in the liver. This is not surprising considering *Noc-/-* mice do not have any obvious alterations in growth or development.

These studies reveal Nocturnin has a profound effect on a wide variety of physiological functions and its function may differ in a tissue specific manner and via its interactions with other genes, as in the example of its partnering with the transcription factor Pparg. Another interesting phenotype that *Noc-/-* mice have is lower body temperature, and this difference becomes more pronounced under a high fat diet (Green et al., 2007). Furthermore, it has been reported Noc-/- mice have some impairments in ex vivo BAT function (Kawai et al., 2010b). In this chapter, I further investigate Nocturnin's role in brown adipose tissue and thermogenesis as well as its role in mitochondrial function.

Results

Nocturnin Displays Dual Localization in the Mitochondria and Cytosol and Noc-/- MEFs Have Impaired Uncoupled Mitochondrial Respiration

Analysis of Nocturnin's amino acid sequence indicates a putative mitochondrial targeting sequence (MTS) at the N-terminus of the protein, as determined by prediction programs (MitoprotII, TargetP and MultiLoc), with >90% prediction scores (Figure 1A). To determine whether Nocturnin is present within the mitochondria, we carried out biochemical fractionation of HEK-293 cells to separate the mitochondrial fraction from the cytosolic fraction, followed by a Proteinase K protection assay on the mitochondrial fraction (Figure 1B). Proteinase K protection was confirmed with the use of MT-CO1 (mitochondrial matrix) as positive control. Nocturnin was protected from degradation upon Proteinase K treatment, confirming that it is localized within the mitochondria. This result confirms a portion of the endogenous Nocturnin is localized within the mitochondria, although further experimentation is necessary to determine its sub-mitochondrial localization.

Two potential translation initiation sites (AUG codons) surround the predicted MTS. However, neither AUG codon is surrounded by an optimal Kozak consensus sequence, raising the possibility of dual translation initiation sites via the leaking scanning mechanism (Kochetov, 2008; Kozak, 2005). Publicly available ribosomal profiling (Ribo-Seq) data show ribosomal enrichment at both initiation sites, in MEF cells and mouse liver. (Gao et al., 2015; Janich et al., 2015). Further, initiation Ribo-Seq experiments confirmed that these alternative

sites are being used for translation initiation in MEFs and in epidermis (Figure 1C)(Lee et al., 2012; Sendoel et al., 2017). We hypothesized that the choice of AUG codon determines whether the MTS is included in the translated protein, thereby dictating whether Nocturnin is localized to the mitochondria or cytoplasm. To test this, I infected Noc-/- MEFs with lentivirus expressing wtNOC or single point mutants NOC(M1A) or NOC(M65A), in order to force translation initiation at the first or second start codon respectively (Figure 1D). As expected, Nocturnin(M1A) localized to the cytoplasm exclusively, whereas Nocturnin(M65A) showed predominant mitochondrial localization as detected by overlap with the mitochondrial stain MitoTracker Red (Figure 1E). Cells expressing wtNOC exhibited both cytoplasmic and mitochondrial localization.

Noc-/- MEFs display impaired uncoupled respiration

In order to determine whether Nocturnin contributes to mitochondrial oxidative phosphorylation, I performed Seahorse XFe96 assays to measure oxygen consumption (Figure 2B). No differences in basal respiration were observed, but there was a mild but significant reduction in uncoupled respiration post-CCCP injection in *Noc-/-* MEFs. CCCP-induced respiration mimics a physiological energy demand situation where mitochondria operate at maximum capacity. In order to confirm that the impairment in the uncoupled respiration is specific to the loss of Nocturnin, I infected *Noc-/-* MEFs with wtNOC or GFP lentiviral constructs. Stable expression of Nocturnin (Figure 2A) was sufficient to rescue the

defect in maximal respiration (Figure 2B), indicating that the phenotype is specific to the loss of Nocturnin.

Nocturnin is Induced with Cold Exposure in Brown Adipose Tissue and Noc-/- Mice Have Alterations in Thermogenesis

Brown adipose tissue (BAT) uses uncoupled mitochondrial respiration to produce heat in response to cold temperatures. An acute cold-exposure protocol (6°C for 4 hours) revealed that Nocturnin was robustly induced in the BAT from WT mice (Figure 3A). Biochemical fractionation indicated that the Nocturnin is present in both cytoplasmic and mitochondrial compartments in BAT at room temperature (Fig. 3B). I hypothesized the *Noc-/-* mice might have a thermogenesis deficit, due to a defect in uncoupled respiration (Fig. 2B). Because Nocturnin expression is robustly circadian with peak levels during the night (Wang et al., 2001), I examined thermogenic responses following cold exposure at two opposite phases of the circadian cycle. WT and *Noc-/-* mice were put in cold chambers at one hour after light onset (ZT1) or one hour after dark onset (ZT13) and temperatures were measured every 4 hours for the following 12 hours. I observed a mild deficit in the thermogenic recovery in the *Noc-/-* mice in both conditions (Fig. 3C). The effect was significant at the daytime group after 8 hrs in cold, whereas in the nighttime group the effect appeared later (after 14 hrs in cold). These results indicate that Nocturnin is not strictly required for cold-temperature adaptation, though cold adaptation mechanisms were less robust in the *Noc-/-* animals. Consistent with this, induction of known cold-responsive genes

were largely intact in *Noc-/-* mice (Fig 3D), although some genes (e.g., Pparg) exhibited reduced responsiveness.

Mitochondrial gene expression is altered in response to cold in the Noc-/- mice.

Considering Nocturnin's role as a deadenylase and its presence in the mitochondria I investigated mitochondrial gene expression in *Noc-/-* mice response to cold. As cold exposure could lead to mitochondrial biogenesis I first measured mitochondrial copy number to ensure differences in mitochondrial-encoded transcript levels are not due to changes in the mtDNA copy number. Quantitation of mtDNA copy numbers indicated no significant differences in the *Noc-/-* BAT at either temperature (Figure 4A). I then analyzed the expression of mitochondrial-encoded mRNAs and rRNAs in mice that were randomly assigned to room temperature (RT) or cold exposure (6°C) conditions for 4 hours. Several mitochondrial RNA species in *Noc-/-* BAT were significantly decreased in response to cold exposure, a phenomenon not seen in WT BAT (Figure 4B). Thus, at this early time point of cold exposure, *Noc-/-* BAT is impaired in maintaining stability of mitochondrial RNA species.

Cold-Induced Downregulation of Glycan Biosynthesis Pathway Genes is Altered in Noc-/- mice

Next, we performed RNA-Seq as an unbiased approach to detect cold-induced changes at the transcriptome level in WT and *Noc-/-* mice. For these experiments we used the same BAT tissue from mice kept at either RT or cold for 4 hours using an acute cold exposure protocol, that was described in the previous section. For the RNA-Seq analysis we used the protein-coding genes (mRNAs) and filtered the transcripts that are consistently low across conditions (see Experimental Procedures for details). We then performed DESeq on the genes that are deemed "expressed", in order to identify differentially expressed genes across conditions. We identified 1703 genes in the WT that were upregulated, and 1546 genes that were downregulated in response to cold. *Noc-/-* mice had 1494 genes that were upregulated and 1169 genes that were downregulated (Figure 5A). When I further investigated the genes that are uniquely changed in WT and *Noc-/-* (Figure 5B), I observed that in *Noc-/-* these genes are evenly distributed between downregulation and upregulation whereas for WT the distribution is skewed towards downregulation. Upon closer look at the genes with highest fold changes in WT, I observed that more than two-thirds of the genes with the highest fold change in the WT were going down (Figure 5C). I was particularly interested in the genes downregulated in the WT but not in the *Noc-/-*, as we predicted some of these genes could be potential targets of Nocturnin. In fact, one of the most significant genes that is downregulated in WT was *Igf1*, previously identified as a Nocturnin target in bone tissue. *B3galt2* and *B4gat1* were also among the most significantly downregulated, both

of which are involved in biosynthesis of carbohydrate moieties of glycolipids and glycoproteins. Next, I performed functional enrichment analysis on the top 500 most significant genes that are downregulated uniquely in the WT (Figure 5D). Surprisingly, the most significant enrichment was in the KEGG metabolic pathway involving glycan biosynthesis and metabolism (Figures 5D and 5E). I also observed alterations in the expression profiles of some genes involved in fatty acid biosynthesis and metabolism (Figure 4E), which was among one of the significant categories based on KEGG pathway analysis of the top 500 most significantly upregulated genes in the WT (Table 1).

Metabolomics analysis reveals alterations in tricarboxylic acid cycle metabolites in Noc-/- mice in response to prolonged cold exposure

In order to determine cold-induced changes in the metabolome of *Noc-/-* and WT mice, we performed metabolic profiling analysis. We did not observe major differences in the metabolome upon 4-hour cold exposure, as determined by LS-MS (Figure 6A). We thought a longer period of adjustment could be necessary for the changes in the metabolome to appear and repeated the metabolomics analysis with a prolonged-exposure cohort that were kept in cold for 7 days (Figure 6B and 7). Metabolite profile of *Noc-/-* BAT exhibited alterations upon prolonged cold exposure. We then performed unsupervised hierarchical clustering on *Noc-/-* group and observed distinct clustering of samples based on temperature (Figure 7A). We performed statistical analysis to identify metabolites that contribute most to the temperature-based clustering, shown as variable importance in projection (VIP) score.

Among the top metabolites were TCA cycle metabolites like succinate and citrate, as well as metabolites involved in glycan synthesis, fatty acid oxidation and choline oxidation (Figure 7B). Next, we performed a more targeted metabolic analysis toward TCA cycle metabolites, using GC-MS. Principal component analysis revealed that metabolic profile of *Noc-/-* in response to cold is distinct while all other conditions cluster together, suggesting altered metabolic response to cold in *Noc-/-* mice (Figure 8A). Strikingly, we observed robust alterations in some key TCA cycle metabolites like pyruvate, succinate, malate and aspartate (Figure 8B and 8C). Most significant changes were observed in pyruvate and succinate: there was a 6-fold decrease in pyruvate and a 10-fold increase in succinate in *Noc-/-* mice upon cold while no major changes were observed for these metabolites in the WT, aside from a minor increase in succinate (less than 2-fold).

Figures

Figure 1. Nocturnin exhibits mitochondrial and cytoplasmic localization via the use of alternative translation initiation sites

(A) Nocturnin contains two potential intiation codons (Met1 and Met65), separated by a mitochondrial targeting sequence. Nucleotides in red show the critical components of the Kozak's sequence: A purine (A or G) at position -3 and a G following the AUG start codon. (B) Proteinase K (Prot.K) protection assay of the mitochondrial fraction from HEK-293 cells. Mitochondrial fractions were treated with Proteinase K (100ug/ml) or Triton-X (1%) and samples were blotted for MT-CO1 (mitochondrial) and TUBULIN (cytoplasmic) as controls. WCL, Whole cell lysate. (C) Diagram showing initiation Ribo-Seq results for Nocturnin in MEFs, epidermis and the global aggregate. Figure taken from publicly available GWIPS-viz database (Michel et al., 2014). (D) Diagram on Nocturnin expression constructs. (E) Noc-/- MEFs expressing exogenous version of Nocturnin were stained with antibodies against MitoTracker (red; mitochondria), FLAG (green; NOCTURNIN) and DAPI (blue; nucleus). Scale bar; 21μm.

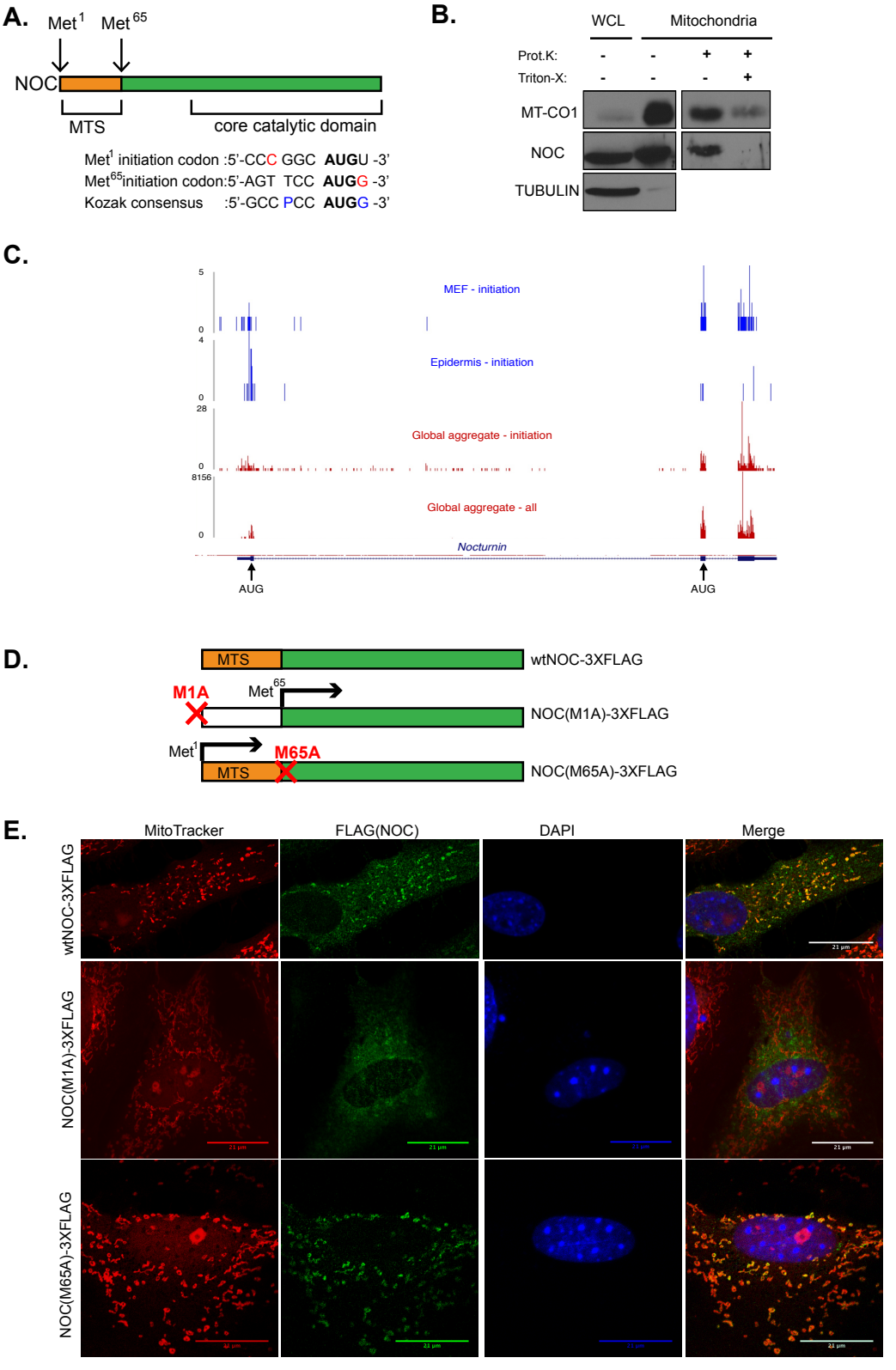
A.
Met1
Met65
NOC
MTS
core catalytic domain
Met1 initiation codon :5'-CCC GGC AUGU -3'
Met65initiation codon:5'-AGT TCC AUGG -3'
Kozak consensus :5'-GCC PCC AUGG -3'
B.
WCL
Mitochondria
Prot.K:
Triton-X:
MT-CO1
NOC
TUBULIN
C.
MEF - initiation
Epidermis - initiation
Global aggregate - initiation
Global aggregate - all
Nocturnin
AUG
AUG
D.
MTS
wtNOC-3XFLAG
M1A
Met65
NOC(M1A)-3XFLAG
Met1
M65A
MTS
NOC(M65A)-3XFLAG
E.
MitoTracker
FLAG(NOC)
DAPI
Merge
wtNOC-3XFLAG
NOC(M1A)-3XFLAG
NOC(M65A)-3XFLAG

Figure 2. Uncoupled respiration is impaired in *Noc-/-* MEFs

(A) Confirmation of stable NOC expression in the Noc-/- MEFs expressing rescue constructs as measured by western blot. (B) (Left) Oxygen consumption rates (normalized to protein concentration) in cells of the indicated genotype. Olig, Oligomycin; CCCP, carbonyl cyanide m-chlorophenylhydrazone; AntA, Antimycin A. (Right) Bar graph showing averages for basal and maximum respiration. Representative experiment from three independent experiments is shown. N=16-23 per group.

****$p<0.0001$, p values are calculated by two-way ANOVA followed by Tukey's post-hoc test. Data are represented as mean ± s.e.m.

A.

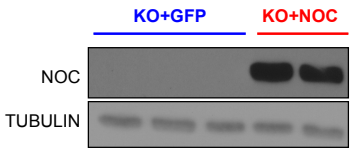
KO+GFP
KO+NOC
NOC
TUBULIN

B.

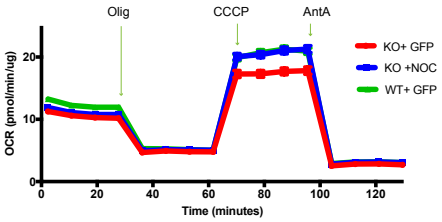
Olig
CCCP
AntA
KO+ GFP
KO +NOC
WT+ GFP
OCR (pmol/min/ug)
Time (minutes)

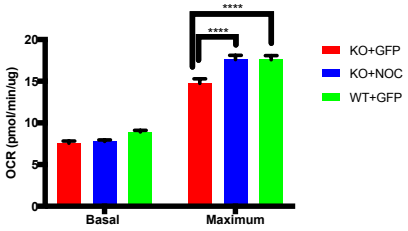
****
****
KO+GFP
KO+NOC
WT+GFP
OCR (pmol/min/ug)
Basal
Maximum

Figure 3. Nocturnin is induced in BAT in response to an acute cold exposure

(A, D) qRT-PCR analysis of BAT samples from WT and *Noc*-/- littermates kept at RT (room temperature) or exposed to cold (6 degrees celcius) for 4 hours. (B) Biochemical fractionation of mitochondrial and cytoplasmic compartments in WT BAT, blotted for NOC, VDAC (mitochondrial outer membrane), MT-CO2 (mitochondrial matrix), ACTIN (cytoplasm) proteins. (C) Core body temperature of mice during prolonged cold exposure at 6 degrees celcius; animals placed at cold at ZT1 (daytime) or ZT13 (nighttime) (N=10/genotype for daytime, N=8/genotype for nighttime group, yellow and black bars indicating day and night respectively). (D) Transcript levels of *Ucp1*, *Pparg*, *Ppargc1a*, *Dio2* genes normalized to *B2M* (N=6 per group for Ucp1, N=4,3 at RT; N=5,4 at Cold, for the rest of the genes). Right panel, RNA-seq analysis of *Noc*-/- and WT littermates (N= 4,4 at RT; N= 5,4 at Cold).

*p<0.05, **p<0.01, ***p<0.001, ****p<0.0001 as analyzed by two-way analysis of variance (ANOVA) with a Tukey's post hoc test (A, D), or two-tailed Student's t-test (C). Data are represented as mean ± s.e.m.

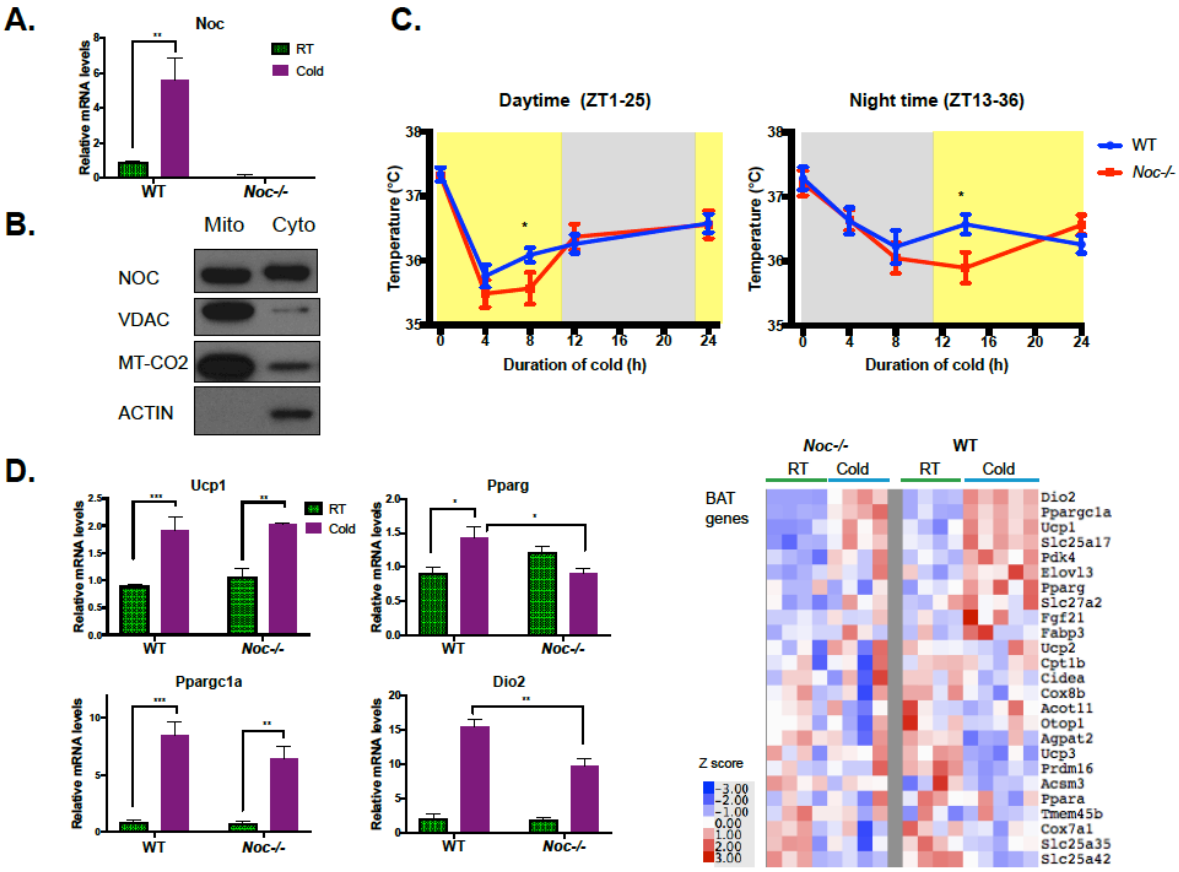
A.
Noc
RT
Cold
Relative mRNA levels
WT
Noc-/-
B.
Mito
Cyto
NOC
VDAC
MT-CO2
ACTIN
C.
Daytime (ZT1-25)
Night time (ZT13-36)
Temperature (°C)
Duration of cold (h)
WT
Noc-/-
D.
Ucp1
Pparg
Ppargc1a
Dio2
Noc-/-
WT
RT
Cold
BAT genes
Z score
Dio2
Ppargc1a
Ucp1
Slc25a17
Pdk4
Elovl3
Pparg
Slc27a2
Fgf21
Fabp3
Ucp2
Cpt1b
Cidea
Cox8b
Acot11
Otop1
Agpat2
Ucp3
Prdm16
Acsm3
Ppara
Tmem45b
Cox7a1
Slc25a35
Slc25a42

Figure 4. Altered mitochondrial gene expression in response to cold in *Noc-/-*

(A) mtDNA copy numbers in BAT of mice kept at RT or cold. (N=4,4 at RT; N=5,4 at Cold). (B) Top, qRT-PCR analysis of mitochondrial-encoded genes in BAT. Transcript levels were normalized to mtDNA copy number (N=4,3 at RT; N=5,4 at Cold). Bottom, average fold changes for mitochondrial genes in response to a 4-hr cold exposure.

*p<0.05, **p<0.01, ***p<0.001, ****p<0.0001 as analyzed by two-way analysis of variance (ANOVA) with a Tukey's post hoc test (A and upper panel in B), or two-tailed Student's t-test (lower panel on B). Data are represented as mean ± s.e.m.

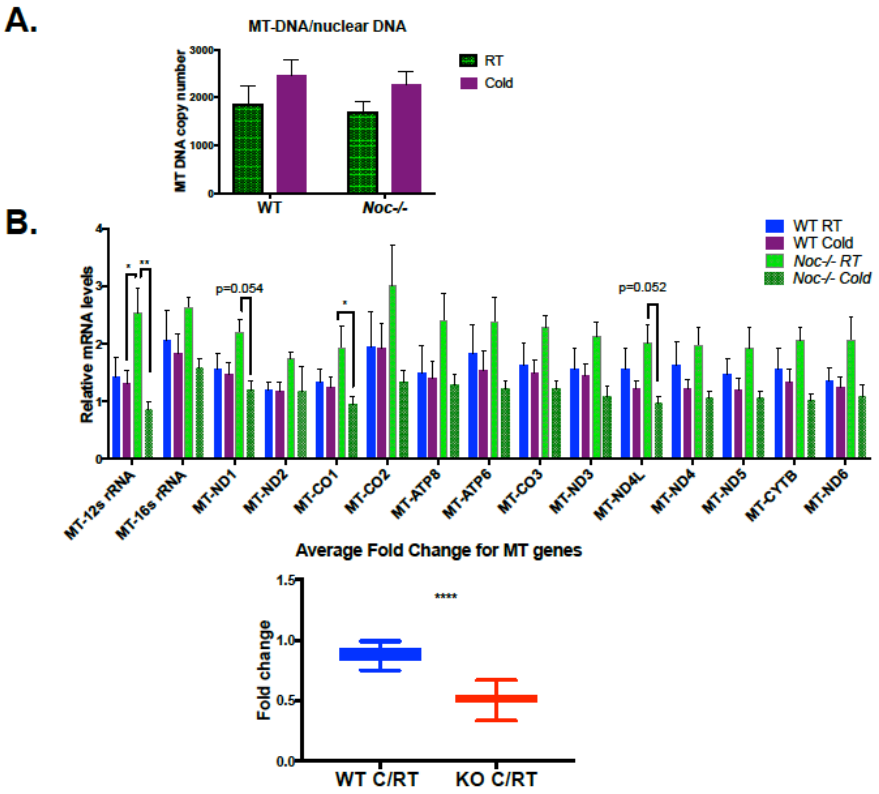
A.
MT-DNA/nuclear DNA
MT DNA copy number
3000
2000
1000
0
RT
Cold
WT
Noc-/-
B.
Relative mRNA levels
WT RT
WT Cold
Noc-/- RT
Noc-/- Cold
p=0.054
p=0.052
MT-12s rRNA
MT-16s rRNA
MT-ND1
MT-ND2
MT-CO1
MT-CO2
MT-ATP8
MT-ATP6
MT-CO3
MT-ND3
MT-ND4L
MT-ND4
MT-ND5
MT-CYTB
MT-ND6
Average Fold Change for MT genes
Fold change
1.5
1.0
0.5
0.0
****
WT C/RT
KO C/RT

Figure 5. Global differences in the transcriptome in response to cold in WT and *Noc-/-* mice

(A) Venn diagrams showing the overlapping and unique genes that are differentially expressed in WT and *Noc-/-* mice BAT tissue. Diagrams showing genes significantly upregulated (left) and downregulated (right) in response to cold (p_{adj}<0.05). Differential mRNA expression between RT and cold conditions in WT and Noc-/- mice was determined by DESeq. Blue, WT; Orange, *Noc-/-*. (B) Volcano plots showing uniquely changing genes in WT (left, blue) and *Noc-/-* (right, red). Log2 fold changes of cold versus RT were plotted against significance values displayed as –log10(p_{adj}). (C) (Left) Waterfall plot showing the distribution of downregulated and upregulated genes in WT. Only genes with absolute log2FC>0.5 are displayed. (Right) Graph showing distribution of downregulated and upregulated genes in WT. Top 100 genes with the highest or lowest Log2 fold change are displayed. (D) Top 500 genes that were uniquely downregulated in WT in response to cold were subjected to functional enrichment analyses using DAVID. KEGG pathway analysis for significantly enriched metabolic categories are shown. (Bottom) KEGG pathway diagram showing which metabolic pathways the genes (red stars) correspond to in the reference pathway map. (E) Heat maps for the differentially expressed genes in glycan biosynthesis and fatty acid metabolism categories. Z scores are shown.

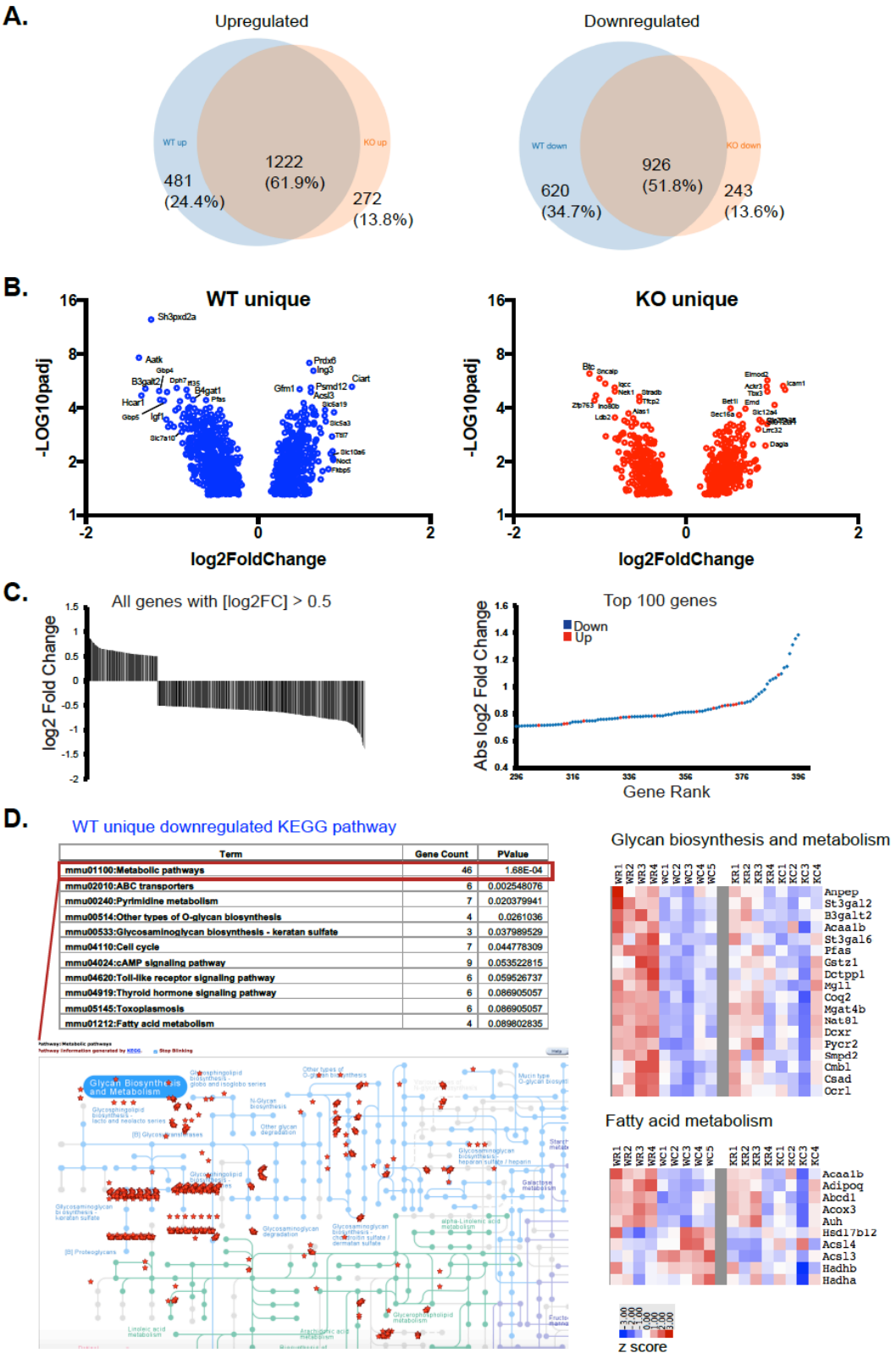
A.
Upregulated
WT up
KO up
481
(24.4%)
1222
(61.9%)
272
(13.8%)
Downregulated
WT down
KO down
620
(34.7%)
926
(51.8%)
243
(13.6%)
B.
WT unique
KO unique
-LOG10padj
log2FoldChange
C.
All genes with [log2FC] > 0.5
log2 Fold Change
Top 100 genes
Down
Up
Abs log2 Fold Change
Gene Rank
D.
WT unique downregulated KEGG pathway
Term
Gene Count
PValue
mmu01100:Metabolic pathways 46 1.68E-04
mmu02010:ABC transporters 6 0.002548076
mmu00240:Pyrimidine metabolism 7 0.020379941
mmu00514:Other types of O-glycan biosynthesis 4 0.0261036
mmu00533:Glycosaminoglycan biosynthesis - keratan sulfate 3 0.037989529
mmu04110:Cell cycle 7 0.044778309
mmu04024:cAMP signaling pathway 9 0.053522815
mmu04620:Toll-like receptor signaling pathway 6 0.059526737
mmu04919:Thyroid hormone signaling pathway 6 0.086905057
mmu05145:Toxoplasmosis 6 0.086905057
mmu01212:Fatty acid metabolism 4 0.089802835
Glycan biosynthesis and metabolism
Anpep
St3gal2
B3galt2
Acaa1b
St3gal6
Pfas
Gstz1
Dctpp1
Mgll
Coq2
Mgat4b
Nat8l
Dcxr
Pycr2
Smpd2
Cmbl
Csad
Ocrl
Fatty acid metabolism
Acaa1b
Adipoq
Abcd1
Acox3
Auh
Hsd17b12
Acsl4
Acsl3
Hadhb
Hadha
z score

Table 1. Gene enrichment analysis for Top 500 most significant WT uniquely upregulated genes

Category	Term	Count	%	PValue	Genes
KEGG_PATH	mmu03013:RNA transport	14	2.9535865	1.78E-04	NUP88, RAN, PAIP1, EIF5B, NXF1, PHAX, EIF2S1, EIF4A2, EIF2S2, DDX20, N
KEGG_PATH	mmu03015:mRNA surveillance pathway	10	2.10970464	4.10E-04	PPP2R1B, PPP2R5B, GSPT1, HBS1L, NXF1, CSTF2T, CPSF2, PPP1CB, DAZAP1
KEGG_PATH	mmu05134:Legionellosis	7	1.47679325	0.00211546	ARF1, VCP, HBS1L, CYCS, NFKBIA, HSPD1, RAB1A
KEGG_PATH	mmu04150:mTOR signaling pathway	7	1.47679325	0.00252675	MAPK1, RHEB, RICTOR, PRKAA2, MTOR, RPS6, PTEN
KEGG_PATH	mmu04152:AMPK signaling pathway	10	2.10970464	0.00300328	PPP2R1B, CD36, PPP2R5B, PPARG, RHEB, FOXO3, PRKAA2, FBP2, MTOR, P
KEGG_PATH	mmu03018:RNA degradation	8	1.68776371	0.00309272	DIS3, CNOT9, PAN3, WDR61, CNOT1, HSPD1, CNOT4, HSPA9
KEGG_PATH	mmu04151:PI3K-Akt signaling pathway	18	3.79746835	0.00371091	PPP2R1B, FLT1, PPP2R5B, MCL1, FLT4, FOXO3, RPS6, PTEN, MAPK1, HSP9(
KEGG_PATH	mmu03050:Proteasome	6	1.26582278	0.00392262	PSMD14, PSMC6, PSMD12, PSMA5, PSMC3, PSMA7
KEGG_PATH	mmu04071:Sphingolipid signaling pathway	9	1.89873418	0.00881674	PPP2R1B, MAPK1, PLCB4, GNAI3, PPP2R5B, ROCK1, SMPD1, PTEN, PPP2R1
KEGG_PATH	mmu04621:NOD-like receptor signaling pathway	6	1.26582278	0.00996608	MAPK1, HSP90B1, ERBIN, NFKBIA, SUGT1, TAB2
KEGG_PATH	mmu01130:Biosynthesis of antibiotics	12	2.53164557	0.01220189	ALDOA, CYP51, ACSS1, SQLE, PLA2G7, FH1, FBP2, PGK1, BPNT1, AK6, HADI
KEGG_PATH	mmu04068:FoxO signaling pathway	9	1.89873418	0.01369714	USP7, MAPK1, SMAD4, BCL6, FOXO3, PRKAA2, AGAP2, CCNG2, PTEN
KEGG_PATH	mmu04144:Endocytosis	14	2.9535865	0.01409546	FLT1, VTA1, ASAP1, CYTH2, RAB7, SMAP1, ARF1, ARPC5L, RAB22A, RAB5A
KEGG_PATH	mmu04120:Ubiquitin mediated proteolysis	9	1.89873418	0.01883589	CUL3, UBE2D3, UBE2A, CUL5, UBA1, KLHL9, NHLRC1, CUL4B, CUL1
KEGG_PATH	mmu04920:Adipocytokine signaling pathway	6	1.26582278	0.02706141	CD36, NFKBIA, PRKAA2, MTOR, ACSL4, ACSL3
KEGG_PATH	mmu01212:Fatty acid metabolism	5	1.05485232	0.03160359	HSD17B12, ACSL4, ACSL3, HADHA, HADHB
KEGG_PATH	mmu05142:Chagas disease (American trypanosoi	7	1.47679325	0.03446341	PPP2R1B, CFLAR, MAPK1, PLCB4, GNAI3, NFKBIA, PPP2R2A
KEGG_PATH	mmu03008:Ribosome biogenesis in eukaryotes	6	1.26582278	0.04579388	CSNK2A2, UTP18, RAN, NOB1, NXF1, AK6
KEGG_PATH	mmu05200:Pathways in cancer	16	3.37552743	0.04749882	GNAI3, ROCK1, PPARG, CYCS, SMAD4, NFKBIA, EGLN1, PTEN, MAPK1, HSP
KEGG_PATH	mmu04919:Thyroid hormone signaling pathway	7	1.47679325	0.05039313	MAPK1, PLCB4, NOTCH4, RHEB, ATP1A1, MED14, MTOR
KEGG_PATH	mmu05152:Tuberculosis	9	1.89873418	0.05617341	MAPK1, LAMP1, CEBPG, CYCS, RAB5A, NFYC, HSPD1, RAB7, HSPA9

Source: DAVID Bioinformatics Resources 6.8

Figure 6. BAT metabolome is altered in response to prolonged cold exposure in *Noc-/-* mice

(A) Heatmap showing average metabolite levels (shown as z-scores) in BAT from WT and *Noc-/-* mice kept at RT or cold (6°C) for 4 hours (N=4-5 per genotype/condition). (B) Heatmap showing z-scores for average metabolite levels in BAT from WT and *Noc-/-* mice upon 7-day cold exposure compared to RT controls (N=4-5 per genotype/condition).

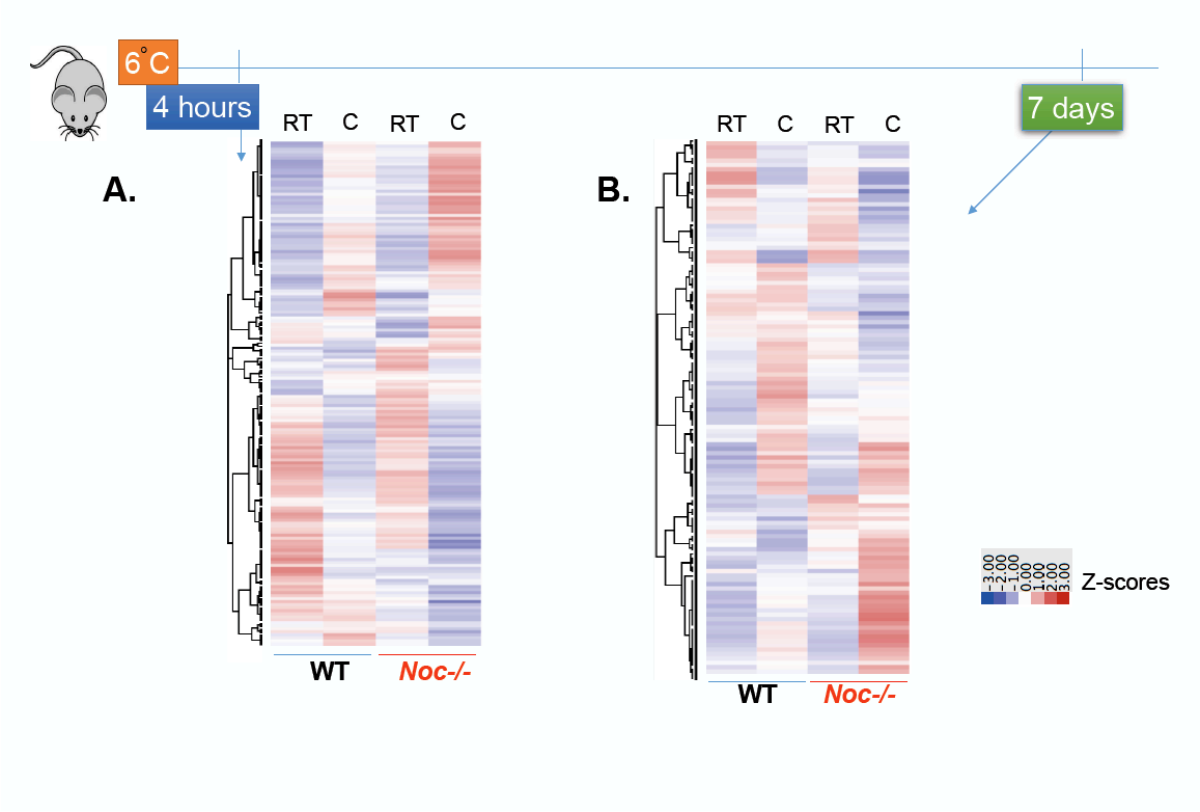
6°C
4 hours
7 days
A.
B.
RT
C
RT
C
WT
Noc-/-
Z-scores

Figure 7. Metabolic profile of *Noc-/-* BAT is altered in response to prolonged cold exposure

(A) Heatmap showing z-scores of the individual metabolite levels in BAT from *Noc-/-* mice kept at RT or at cold (6°C) for 7 days. Samples were clustered using unsupervised hierarchical clustering. (B) VIP scores for top metabolites altered in *Noc-/-* ranked from the biggest to smallest score. Blue and red bars indicate upregulation (blue to red) or downregulation (red to blue) in response to cold. VIP, variable importance in projection.

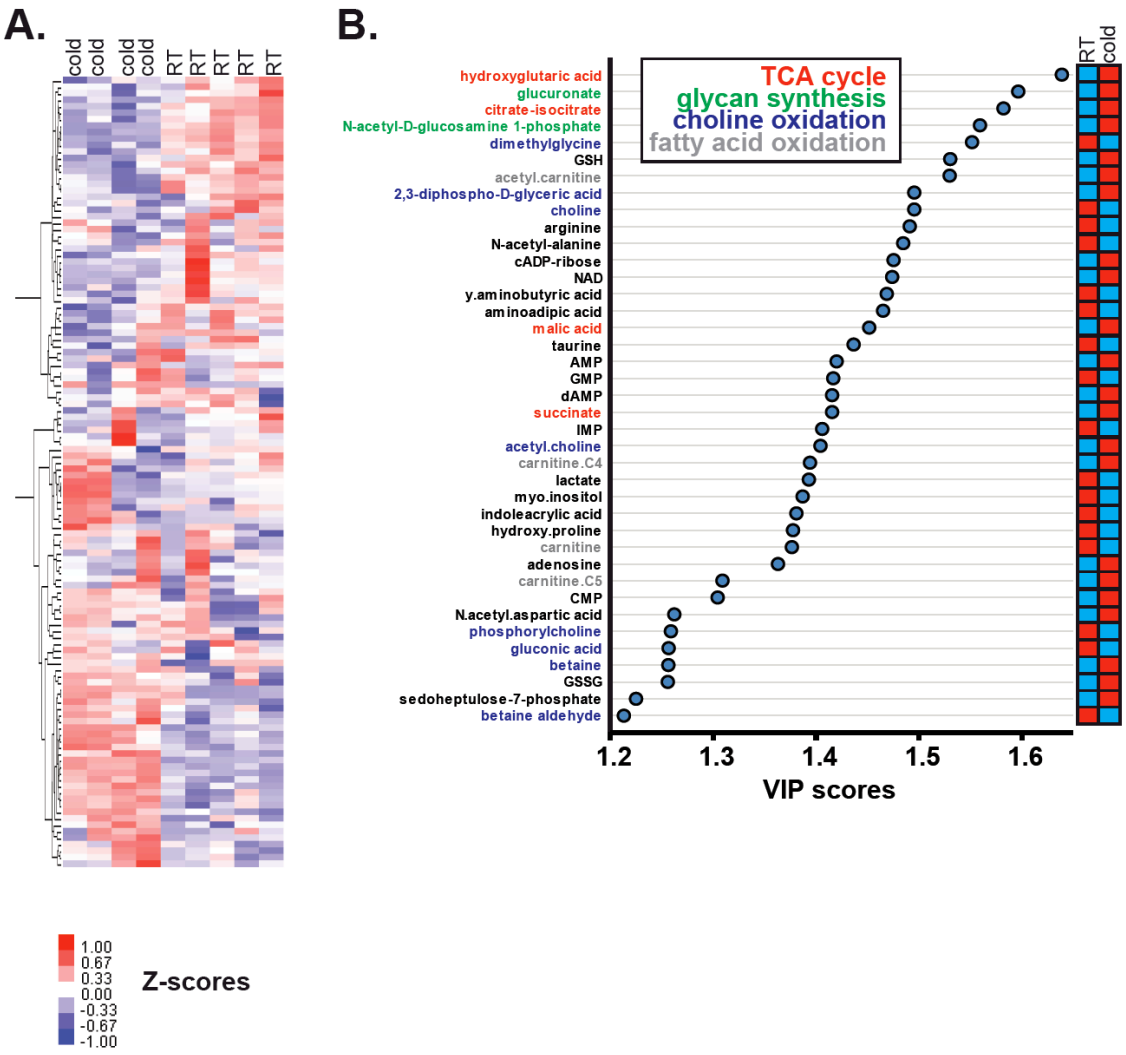
A.
cold
cold
cold
cold
RT
RT
RT
RT
RT
1.00
0.67
0.33
0.00
-0.33
-0.67
-1.00
Z-scores
B.
RT
cold
TCA cycle
glycan synthesis
choline oxidation
fatty acid oxidation
hydroxyglutaric acid
glucuronate
citrate-isocitrate
N-acetyl-D-glucosamine 1-phosphate
dimethylglycine
GSH
acetyl.carnitine
2,3-diphospho-D-glyceric acid
choline
arginine
N-acetyl-alanine
cADP-ribose
NAD
y.aminobutyric acid
aminoadipic acid
malic acid
taurine
AMP
GMP
dAMP
succinate
IMP
acetyl.choline
carnitine.C4
lactate
myo.inositol
indoleacrylic acid
hydroxy.proline
carnitine
adenosine
carnitine.C5
CMP
N.acetyl.aspartic acid
phosphorylcholine
gluconic acid
betaine
GSSG
sedoheptulose-7-phosphate
betaine aldehyde
1.2
1.3
1.4
1.5
1.6
VIP scores

Figure 8. Tricarboxylic acid cycle intermediates are altered in Noc-/- mice in response to prolonged cold exposure

(A) Principal component analysis (PCA) plot for the metabolites from GC-MS analysis. *Noc-/-* and WT mice were kept at RT or cold (6°C) for 7 days. RT, room temperature (B) Box plot analyses showing the median, 25^{th} and 75^{th} percentiles and the range for metabolite levels in *Noc-/-* and WT mice at RT or cold conditions. N=4-5 per genotype. (C) Diagram showing TCA cycle intermediates that are altered in *Noc-/-*. Metabolites altered in the *Noc-/-* are highlighted with red. Red arrows show the intensity and direction of the alteration. *p<0.05, **p<0.01, ***p<0.001, as analyzed by two-tailed Student's t-test.

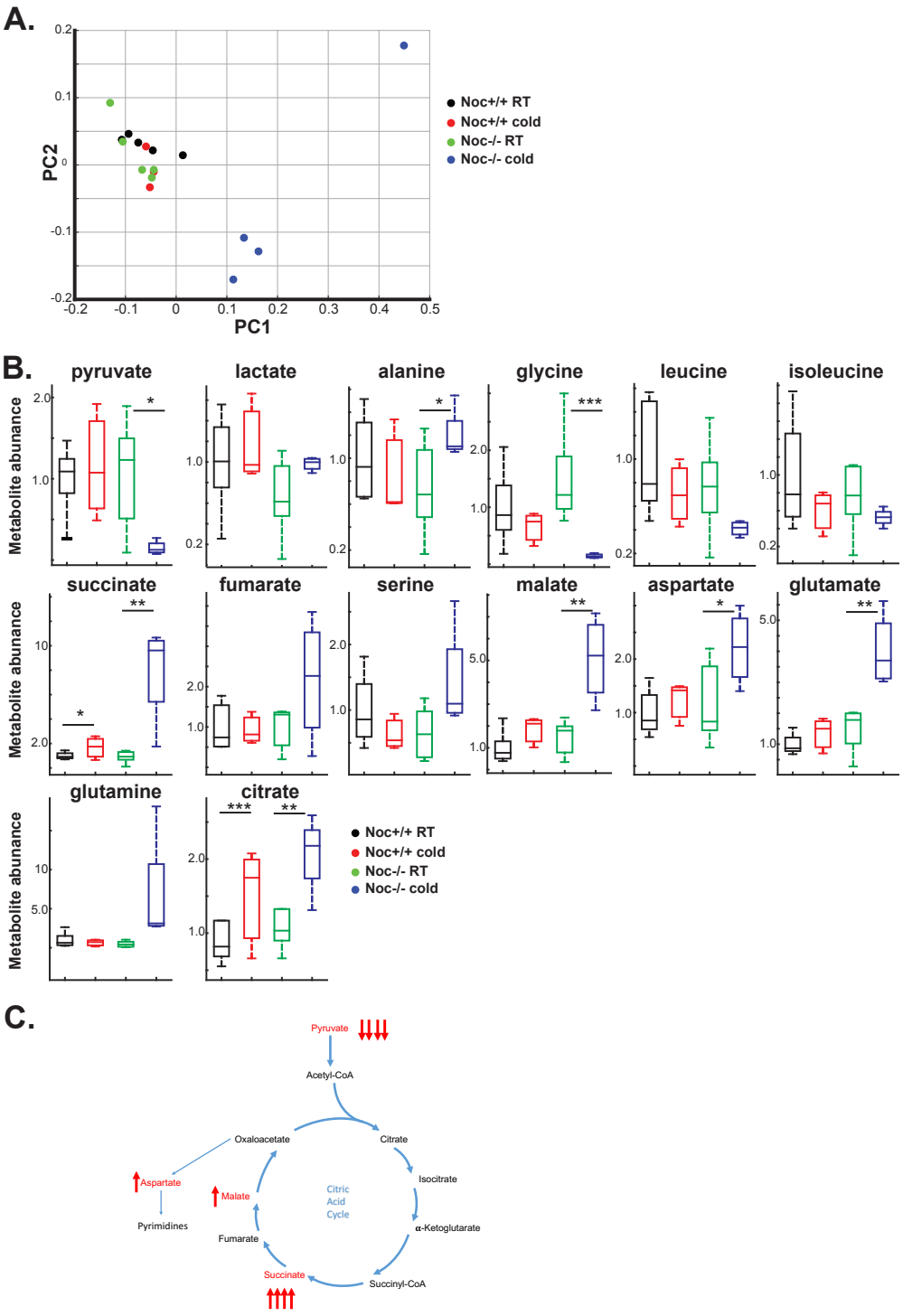
A.
PC1
PC2
Noc+/+ RT
Noc+/+ cold
Noc-/- RT
Noc-/- cold
B.
pyruvate
lactate
alanine
glycine
leucine
isoleucine
succinate
fumarate
serine
malate
aspartate
glutamate
glutamine
citrate
Metabolite abunance
C.
Pyruvate
Acetyl-CoA
Citrate
Isocitrate
α-Ketoglutarate
Succinyl-CoA
Succinate
Fumarate
Malate
Oxaloacetate
Aspartate
Pyrimidines
Citric Acid Cycle

Figure 9. Nocturnin as a metabolic switch in response to cold

Proposed model. Nocturnin acts as a metabolic switch upon cold-exposure by diverting glucose and fatty acids towards the mitochondria. This is achieved by downregulation of pathways like glycan biosynthesis that could utilize glucose under standard conditions.

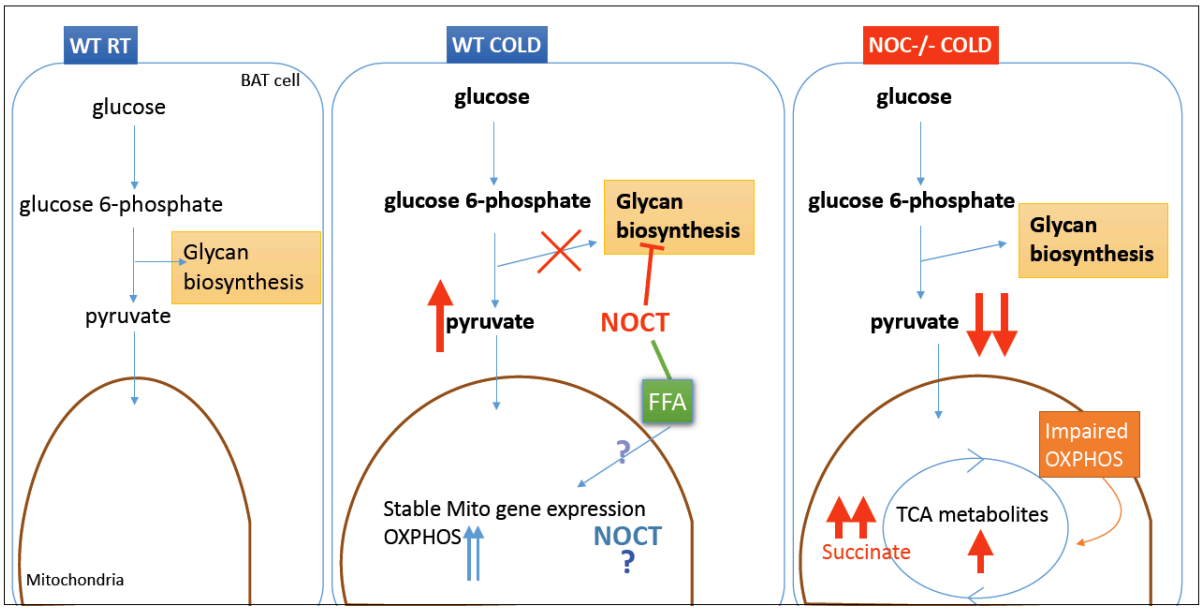
WT RT
BAT cell
glucose
glucose 6-phosphate
Glycan biosynthesis
pyruvate
Mitochondria
WT COLD
glucose
glucose 6-phosphate
Glycan biosynthesis
pyruvate
NOCT
FFA
?
Stable Mito gene expression
OXPHOS
NOCT
?
NOC-/- COLD
glucose
glucose 6-phosphate
Glycan biosynthesis
pyruvate
Impaired OXPHOS
TCA metabolites
Succinate

Discussion

Our results show that Nocturnin is present in mitochondria and has a functional mitochondrial targeting signal that is sufficient for localization to the organelle. I have also shown that Nocturnin is acutely induced in response to cold exposure in mouse BAT, and *Noc-/-* mice have alterations in thermogenesis. Analysis of BAT transcriptome revealed cold-induced remodeling of glycan biosynthesis pathway genes as well as some lipid metabolism genes, which is perturbed in *Noc-/-* BAT. I also observed that *Noc-/-* mice are impaired in maintaining stability of mitochondrially encoded genes upon cold exposure. Lastly, metabolomics analysis revealed robust alterations in a number of key tricarboxylic acid (TCA) cycle metabolites upon a longer 7-day cold exposure paradigm. One caveat of this study is that we compared RT vs cold, and RT is known to be sub-thermoneutral for mice. Thus, it should be noted that our comparison here is between slightly activated (RT) and robustly activated (cold) BAT.

Two major fuel sources for BAT are glucose and free fatty acids (FFAs), which are metabolized in mitochondria at high rates upon cold exposure in order to generate heat. We propose a model whereby Nocturnin acts as a metabolic switch in response to cold exposure: it is induced rapidly and diverts glucose for oxidation in the mitochondria by downregulating glycan biosynthesis enzymes such as *B3galt2* and *B4gat1* (Figure 9). There are also alterations in some FFA metabolic genes in *Noc-/-* BAT in response to cold: *Acsl3* and *Acsl4* are upregulated in WT but not in *Noc-/-* animals. *Acsl3* and *Acsl4* are implicated in long chain fatty acid activation, thus, we propose that Nocturnin may also be responsible for

diverting FFAs to the mitochondria in response to cold; possibly through interactions with lipid metabolism genes such as Pparg. This idea is consistent with the increased NEFA and triglycerides in the circulation of *Noc-/-* mice, that suggest reduced uptake by specific organs (Stubblefield et al., 2018). Importantly, we observed a robust decrease (around 7-fold) in pyruvate in response to a prolonged cold exposure in *Noc-/-* mice, while WT mice maintained their pyruvate levels. This depletion in pyruvate supports the idea of impaired fuel availability in knockout BAT, as a result of dysregulated metabolism.

Uncoupled respiration was decreased in *Noc-/-* MEFs, and rescued by lentiviral expression of Nocturnin. In BAT, we observed a reduction in the mitochondrial genome-encoded mRNAs in *Noc-/-* mice in response to cold, while WT mice were able to maintain the stability of these mRNAs. This was surprising, as it suggests Nocturnin helps maintain the stability of mitochondrial genes – an opposing effect than expected if Nocturnin acts as a deadenylase. Although Nocturnin has deadenylase function in vitro, many studies have identified Nocturnin's in vivo role as much more complex. For instance, Nocturnin was shown to be necessary for the stabilization of *iNOS* mRNA (Niu et al., 2011). Nocturnin was also shown to interact with PPARγ and to promote adipogenesis in 3T3-L1 cells by stimulating its nuclear translocation (Kawai et al., 2010b). One possibility is that Nocturnin interacts with transcription factors in the mitochondria and promote mitochondrial mRNA stability indirectly. Lastly, there have been conflicting reports in the literature about the role of polyadenylation on mitochondrial mRNA stability (Nagaike et al., 2005; Nagao et al., 2008; Piechota et al., 2006; Rorbach and Minczuk, 2012; Rorbach et al., 2011; Tomecki et al., 2004). Two recent studies did not report changes in poly(A) tail length or stability in the

knockout of mitochondrial deadenylase PDE12 (Bratic et al., 2016; Pearce et al., 2017). Yet, they reported aberrant adenylation in non-coding mt-tRNAs which effects proper translation.

We also observed robust alterations in some key tricarboxylic acid cycle metabolites in *Noc-/-* upon a 7-day cold exposure. Most significantly, there was a striking 6-fold decrease in pyruvate and 10-fold increase in succinate in the *Noc-/-* cold BAT, while no major differences for these metabolites were observed in the WT, aside from a slight increase in succinate (less than 2-fold). Malate and aspartate, other TCA cycle intermediates were also elevated in the *Noc-/-* BAT. This depletion of pyruvate and alteration of citric acid intermediates could explain the deficit in the *Noc-/-* uncoupled respiration, and is also consistent with the reduced hepatic ATP levels previously reported in *Noc-/-* mice (Kojima et al., 2015). These results, however, are inconsistent with the metabolic cage data from *Noc-/-* mice, showing increased metabolic rate in these mice upon high-fat diet (Stubblefield et al., 2018). Tissue specific effects of Nocturnin could be one explanation, as previously mentioned.

The increase in succinate is interesting as succinate was shown to be an indicator of reactive oxygen species (ROS) production (Chouchani et al., 2014). The increase in succinate levels has been previously observed in mtDNA mutant cells (Mullen et al., 2014), and succinate-drived respiration is mediated by complex II, which is completely encoded by the nuclear genome. Thus, the metabolic changes in the *Noc-/-* mice are generally consistent with decreased consumption of TCA cycle metabolites, and a shift to complex II dependent respiration – a phenomenon often seen in mtDNA disease. Future experiments utilizing

isotopic tracing techniques to quantitate the fate of glucose may elucidate the metabolic pathway alterations present in Noc-/- BAT.

In conclusion, our findings suggest Nocturnin has an important role in mediating the short-term and long-term metabolic adaptations in response to cold in BAT. Whether these adaptations are through Nocturnin's deadenylase function or if there are other novel functions of Nocturnin in vivo is yet to be explored.

Experimental Model and Subject Details

Animal Studies

Male and female WT and *Noc-/-* C57BL/6 (congenic, N>9) mice were group-housed, under standard laboratory conditions, including a 12-hr light/dark cycle and free access to regular chow (Harlan Teklad diet 2918) and water.

For cold exposure experiments, age-matched 10-20 week old young adult WT and *Noc-/-* mice were randomly assigned to cold (6°C) or room temperature (22°C) groups. Mice were single housed for the duration (4hrs) of the experiment and food was removed in order to minimize individual variation. For the 7-day cold exposure protocol, WT and *Noc-/-* mice were single housed at 6°C for the duration of the experiment with free access to food and water. At the end of the experiment mice were killed by decapitation and BAT was dissected and immediately frozen in liquid nitrogen and stored at -80°C. All animal studies were conducted in accordance with IACUC regulations and guidelines.

Plasmids and Cell lines

To generate the Noc-FLAG lenti virus construct, the mouse Nocturnin cDNA with 3x flag tag was subcloned into the Age1 and EcorR1 sites of pLJM1-EGFP. pLJM1-EGFP plasmid was obtained from Addgene (Plasmid#19319). Single point mutants were made using Q5 Site-Directed Mutagenesis Kit according to manufacturer's instructions by some

modifications. Briefly exponential amplification was performed with PCR using the primers with the point mutations mNOC (M1A), mNOC (M65A) and the template plasmid (pLJM1-mNOC). Next day, Kinase, Ligase& Dpnl (KLD) treatment was performed with some modifications. Instead of using 10X KLD enzyme mix, 1µl Quick ligase, T4 PNK and Dpn1 were individually added to the mixture. Next, transformation was performed using DHSα competent cells according to manufacturer's instructions, using ampicillin selection plates. After overnight incubation at 37°C, colonies were selected and bacterial cultures were grown with LB and the selection marker. Plasmid DNA was isolated using QIAprep Spin Miniprep Kit (Qiagen). Plasmid DNA was then sent to sequencing for the confirmation of the point mutations.

Lentiviral particles were produced according to Addgene protocol. Briefly, pLJM1-EGFP, pLJM1-NOC, pLJM1-NOC(M1A) and pLJM1-NOC(M65A) plasmids were mixed with packaging and envelope plasmids and with FUGENE Transfection Reagent (Promega) in serum-free OPTI-MEM, so that FUGENE: total DNA ratio will be 3:1. 50-80% confluent HEK-293T cells (in DMEM that does not contain antibiotics) were then transfected with this mixture. Cells were incubated at 37°C, 5% CO_2 for 12-15 hours. Next morning, transfection reagent was removed and replaced with fresh media (DMEM+10%FBS+penicillin/strepromycin). Cells were incubated for another 24 hrs at 37°C, 5% CO_2. On Days 4 and 5, lentiviral particles were collected and stored at -80 until use.

Generating Stable Cell Lines

70% confluent MEF cells were infected with 0.1-1mL lentiviral particles with the constructs. Polybrene (8μg/ml) was added to the media to increase viral infection efficacy. Titration was performed in order to assess the infection efficacy and to decide the optimal concentration of lentiviral particles for the desired gene expression level. Cells were incubated overnight and changed to fresh media after 24 hrs and selected with puromycin. Lentiviral infection was visually confirmed for the pLJM1-GFP construct and western blotting was performed to confirm the expression of the other target genes.

Methods

Temperature Measurements

WT and *Noc-/-* mice were gender-matched so that there are equal number of male and female for each genotype. Mice were single housed at 6°C with free access to food and water for the duration of the experiment and core body temperature was measured by a rectal thermometer.

qRT-PCR

Total RNA was extracted from BAT tissue by Trizol (Invitrogen) using a dounce homogenizer (Wheaton). 1ug of total RNA was used to make complementary DNA using the High-Capacity cDNA Reverse Transcription kit (Applied Biosystems). Diluted cDNAs (1/100) were amplified by Power SYBR Green Master Mix (Applied Biosystems) using gene specific primers. Relative mRNA levels were calculated by quantitative PCR method and normalized to B2M gene.

RNA-seq

mRNA-seq libraries were prepared as previously described (Takahashi et al., 2015). Sequencing was performed by Nextseq Sequencing System (Illumina) on individually barcoded samples. Average sequencing depth was 55 million reads/sample. Raw gzipped fastq reads of length 76 nucleotides from the Illumina Nextseq machine were further compressed using clumpify program from BBMap Suite version 37.55. This step leaves the raw data unchanged, but implements a sorting technique based on the fastq sequence to that the order of sequences is changed to yield better compression in terms of storage and faster processing times for the aligner. Using fastqc, the reads were checked for quality followed by treatment with an in-house python script to trim low quality reads. These python script trimmed reads were further trimmed with cutadapt using parameters "-g AATGATACGGCGACCACCGAGATCTACACTCTTTCCCTACACGACGCTCTTCCGA

TCT -a AGATCGGAAGAGCACACGTCTGAACTCCAGTCAC -m 30". Another round of fastqc is implemented to check the post-trimmed read quality distributions. These two step trimmed fastq files are given as input to STAR for alignment, against M14 annotation of GENCODE, with parameters "--readFilesIn input.trim.gz --readFilesCommand zcat --sjdbGTFfile M14.annotation.gtf --outFilterType BySJout --outFilterMultimapNmax 10 --alignSJoverhangMin 10 --alignSJDBoverhangMin 1 --outSAMtype BAM SortedByCoordinate --outSAMunmapped Within --outFilterMismatchNmax 3 --twopassMode Basic". The resultant BAM file was filtered for ribosomal RNA and secondary alignments by keeping the uniquely mapped reads. Coverage tracks were generated using in-house python script by normalizing each sample to 10million total reads. HTSEQ was used for raw read counting and RPKM was calculated using an R script. Low expressing transcripts across conditions were filtered by setting a RPKM cutoff of > 0.5 for the average of all conditions. The raw read counts from HTSEQ count were used to identify differentially expressed genes using DESEQ2. Differentially expressed genes with an FDR < 0.05 are considered significant.

Cell Culture

Human embryonic kidney 293 (HEK293) and immortalized mouse embryonic fibroblast (MEF) cell lines were maintained in high-glucose DMEM supplemented with 100U/ml penicillin, 10μg/ml streptomycin and 10% fetal bovine serum.

Immunocytochemistry and Confocal Microscopy

Standard immunocytochemistry protocol was used. Briefly, cells were washed twice with PBS and then incubated with 300nM MitoTracker Red CMXRos for 30 minutes at 37°C. Cells were then washed once with PBS and fixed with 4%PFA at 37°C for 10 minutes. They were then washed 3 times with PBS and permeabilized with 0.2% TritonX/PBS for 10 minutes. Cells were then blocked with 3%BSA/PBS for 30 minutes and incubated overnight with the primary antibody added to the blocking solution. Next day, cells were washed 3 times with PBS and incubated with the secondary antibody AlexaFluor 488 (Life technologies). Cells were then washed 3 times with PBS and incubated 5 min with DAPI. After another wash cells were mounted into coverslips. PBS washes were 5 minutes each. Confocal images were acquired using Zeiss LSM 710 and images were analyzed using Zen software.

Mitochondrial Respiration Assay

Cellular respiration was measured using the Seahorse XFe 96 analyzer (Seahorse Biosciences, Agilent technologies). Briefly, 14000 cells were plated into micro well plates the night before the assay. Next day, cells were washed and cell culture media was replaced by assay media (DMEM (Sigma D5030) supplemented with 10%FBS, 1%penicillin/streptomycin, 2mM glutamine, 1mM pyruvate, 10mM glucose). Cells were adjusted to the assay media for one hour at 37°C before the experiment. Seahorse cartridge

was loaded with assay drugs and the assay was run. The final concentrations for the drugs that were used in the experiment were: oligomycin (2μM), CCCP (10μM) and antimycinA (2μM). Protein concentrations were calculated using BCA assay kit (ThermoFisher).

DNA Extraction

Mitochondrial and genomic DNA was extracted from BAT tissue using DNeasy Blood and Tissue Kit (QIAGEN) according to manufacturer's instructions. 10ng of DNA was then amplified by qRT-PCR using primers for genomic and mitochondrial DNA.

Mitochondrial Fractionation and Proteinase K Assay

Mitochondrial isolation was performed as previously described (Frezza et al., 2007). Briefly, five confluent 10cm plates of HEK 293 cells were collected using a cell scraper, then resuspended in 3ml of isolation buffer. Approximately 1,000,000 cells were collected, spun down, and lysed in 100ul of RIPA buffer for the whole-cell lysate. The rest of the cell suspension was mechanically disrupted using a glass-Teflon dounce homogenizer. The lysates were spun down at 600g for 10 minutes at 4C to pellet unbroken cells and nuclei. The supernatant was collected and centrifuged again at 7,000g for 10 minutes at 4C to pellet the mitochondrial fraction. The mitochondrial pellet was washed with 200ul of isolation buffer and then equally split into 7 different microcentrifuge tubes. The pellet was spun down at 7,000g for 10 minutes at 4C, and the supernatant was discarded. The mitochondrial pellets

were resuspended in 40ul of reaction buffer. Briefly, 100μg/ml Proteinase K and/or 1%TritonX-100 were added to the samples in isolation buffer and samples were incubated on ice for 30 minutes. The reaction was stopped by the addition of 2ul of 100mM PMSF and 10ul of 5x SDS sample buffer. Ten microliters of each sample were loaded for SDS-PAGE and Western blot analysis, probing for Tubulin, Nocturnin, and MT-CO1 (positive control).

BAT Metabolomics

Frozen BAT tissue (50-100mg) was homogenized in choloroform/methanol/H_2O (40:40:20), and metabolites were extracted from the polar layer. Samples were subjected to three freeze-thaw cycles, and spun at 14000rpm for 15min to pellet precipitants. The supernatant was transferred to a new tube and evaporated overnight. For GC-MS measurements, dried metabolites were derivatized to form methoxime-TBDMS derivates by incubating with 1% methoxyamine hydrochloride (Sigma-Aldrich) in pyridine at 70C for 15 minutes followed by addition of *N*-*tert*-Butldimethylsiyl-*N*-methyltrifluoroacetamide (MTBSTFA, Sigma-Aldrich) for 1 hour. Derivatized samples were analyzed by using an Agilent Technologies 7890B gas chromatographer with a HP-5MS 5% phenyl methyl Silox column (30 m x 250 um x 0.25 um, Agilent) coupled to an Agilent Technologies 5977A mass spectrometer. The injector was operated in splitless mode at 280C. The oven was set at 60C, held for 1 minute, then 10C/min to 320C and held for 1 minute. The mass spectrometer was set to scan from 75 – 1000 *m/z*. Integrated peak areas for each metabolite were normalized by total ion count. For LC-MS/MS measurements, dried metabolites were resuspended in 0.03% formic acid,

vortexed and centrifuged to remove debris. Samples were randomized and blinded prior to analysis on an AB QTRAP 5500 liquid chromatograph/triple quadropole mass spectrometer (Applied Biosystem SCIEX). Chromatogram review and peak area integration was performed in MultiQuant software. Peak areas were normalized against the total ion count.

CHAPTER THREE

ANALYSIS OF NOCTURNIN'S FUNCTION IN THE SYNAPSE

Introduction

Activity-dependent local translation in the dendrites is considered to be an important component of synaptic plasticity underlying learning and memory. Thus, rapid dendritic translation has been shown to be necessary for some forms of protein-synthesis dependent synaptic plasticity like long-term potentiation (LTP) and long-term depression (LTD) (Bramham and Wells, 2007). One of the well-documented cases of this is group I metabotropic receptor-dependent LTD (mGluR-LTD) (Huber et al., 2000; Waung et al., 2008).

For local translation, dendritic mRNAs are thought to be transported to the synapse at a translationally suppressed state and get translated upon synaptic activation (Holt and Schuman, 2013; Krichevsky and Kosik, 2001). To date, many dendritic mRNAs to be regulated in this way have been identified, like Arc, αCaMKII and FMR1 (Bramham and Wells, 2007). Growing evidence suggest specific subsets of these mRNAs might be required for different forms of plasticity which raises the questions of how these mRNAs are regulated at an individual level and what determines which mRNAs to be translated or to remain suppressed.

One possible mechanism for the differential regulation of dendritic mRNAs in the synapse is through post-transcriptional mechanisms like polyadenylation and deadenylation. In fact, there is evidence showing bidirectional regulation of synaptic plasticity via polyadenylation and deadenylation (Kim and Richter, 2006; Udagawa et al., 2012; Wells et al., 2001). Briefly, cytoplasmic-polyadenylation-element-binding protein 1 (CPEB1) forms a complex that involves deadenylase PARN and polyA polymerase Gld2. Upon neuronal activation, PARN is dispelled from the complex which allows Gld2 to polyadenylate target mRNAs that leads an increase in their translation (Udagawa et al., 2012).

Nocturnin is an RNA-specific nuclease, a circadian deadenylase first discovered in the retina of *Xenopus laevis* (Green and Besharse, 1996), and is conserved among eukaryotes. According to in-situ hybridization studies, Nocturnin is expressed widely throughout the different regions of the brain, one of which is hippocampus (Lein et al., 2007; Wang et al., 2001). Nocturnin is also an immediate early gene, that is acutely induced by a variety of stimuli (Garbarino-Pico et al., 2007; Kawai et al., 2010b; Niu et al., 2011). All these considered, we hypothesized that Nocturnin might have a role in the post-transcriptional regulation of dendritic mRNAs. In this chapter I analyzed Nocturnin's localization in the neurons and its potential role in synaptic plasticity. Considering its wide expression profile in the brain, I also analyzed if *Noc-/-* mice have any alterations in behavior (See Appendix).

Results

Nocturnin is Localized in the Cytoplasm and the Dendrites in Neurons

I investigated the subcellular localization of Nocturnin in primary neuronal cultures as well as in brain slices from mice (Figure 1A and 1D). First, I examined the localization of endogenous Nocturnin in cultured cortical neurons that were fixed at days in vitro (DIV) 6 to DIV10 and imaged by confocal microscopy. I observed that Nocturnin is localized in the perinucleus and cytoplasm as well as in the neuronal processes starting from early development stages of the neuron throughout maturity (Figure 1A). Next, I analyzed Nocturnin localization in brain slices utilizing a mouse model with forebrain-specific overexpression of Nocturnin. Briefly, I bred transgenic mice expressing tetracycline controlled transactivator protein (tTA) under CamK2 promoter (CamK2a-tTA+ mice) with another transgenic strain that have Noc-Flag coupled to a tetracycline-responsive promoter element (TRE-NocFlag+ mice) to generate CamK2a-tTA+/-; TRE-Noc-Flag+ mice (Figure 1B). Forebrain specific overexpression of NOC-FLAG was confirmed by western blot. To examine if Nocturnin is present in the dendrites, I imaged cortical brain slices from these mice that I stained with an antibody against FLAG to detect NOC-FLAG and with MAP2 antibody as a dendritic marker. I observed some overlay between FLAG and MAP2 signal suggesting overexpressed Nocturnin is present in the dendrites (Figure 1D). Antibody specificity was confirmed by staining brain slices from transgene negative mice. I also imaged hippocampal slices and observed FLAG-NOC staining in the apical dendrites of the

CA1 neurons (Figure 1E). To confirm the immunocytochemistry results biochemically, I performed subcellular fractionation from the hippocampus tissue of *Noc-/-* and WT mice. Nocturnin was present in both cytosolic and presynaptic compartments and it was enriched in the post-synaptic density (PSD). Interestingly, I observed that Nocturnin had a second upper band in the post-synaptic fraction suggesting Nocturnin might be post-translationally modified in the PSD.

Analysis of mGluR-LTD in the Schaffer Collateral-CA1 Synapses in Noc-/- Mice

As I confirmed Nocturnin is in the post-synaptic densities in the hippocampus, I examined if Nocturnin has a role in hippocampal mGluR-LTD, which is a protein synthesis-dependent form of synaptic plasticity that requires rapid dendritic translation (Huber et al., 2000). I prepared hippocampal slices from 4-5 week old mice and measured extracellular field potentials (fEPSPs) in the stratum radiatum region of CA1 neurons elicited by Schaffer collateral stimulation (Figure 2A). mGluR-LTD was induced by bath application of mGlur1/5 agonist (RS)-3,5-dihydroxyphenylglycine (DHPG). I observed a significant attenuation of mGluR-LTD in the Noc-/- mice in our first cohort of mice (Figure 2B). The acute depression of fEPSPs measured 4-7 min after the onset of DHPG application was also reduced in *Noc-/-* mice ($p<0.05$). Conversely, I was not able to repeat this phenomenon in a separate cohort (Figure 2C). These conflicting results could be due to different anesthetics used in these cohorts. (see Discussion).

Basal Synaptic Transmission and Short-Term Plasticity Are Not Altered in Noc-/- Mice

In order to analyze basal synaptic properties, I generated input-output(I/O) curves by measuring fEPSP amplitude for increasing stimulus intensities. There were no significant differences between the I/O curves of *Noc-/-* and WT mice, indicating basal synaptic transmission is not altered in *Noc-/-* mice. I also examined short-term plasticity by measuring paired pulse facilitation (PPF) which is an indicator of presynaptic release probability. Briefly, the ratio of fEPSPs elicited in response to two pulses with varying interstimulus intervals is calculated. There were no differences in PPF between genotypes, indicating *Noc-/-* mice have no alterations in neurotransmitter release probability.

Figures

Figure 1. Analysis of subcellular localization of Nocturnin in neurons

(A) Cultured cortical neurons from E16 embryos were fixed with 4% paraformaldehyde (PFA) at DIV 6 through DIV10 and processed for immunofluorescence using Nocturnin antibody. DIV, Days in vitro. (B) Breeding scheme showing the generation of the CamK2a-tTA+/-; TRE-Noc-Flag+ mice for the forebrain-specific overexpression of FLAG tagged Nocturnin. (C) Representative western blot showing biochemical fractionation for isolating the different compartments from *Noc-/-* and Noc+/+ hippocampal tissue. Input, Total homogenate; Sup1, Cytosolic compartment; Sup2, Presynaptic compartment; PSD, Post synaptic density. (D) CamK2a-tTA+/-; TRE-Noc-Flag+ and CamK2a-tTA-/-; TRE-Noc-Flag+ mice were transcardially perfused with 4%PFA and brain slices were stained for FLAG and the dendritic marker MAP2. Representative confocal images from the cortex are shown. Arrowheads show the overlay of FLAG and MAP2. (E) Representative confocal images showing FLAG staining in the hippocampus. All confocal images were taken using 63X oil immersion objective. Scale bar, 22μm.

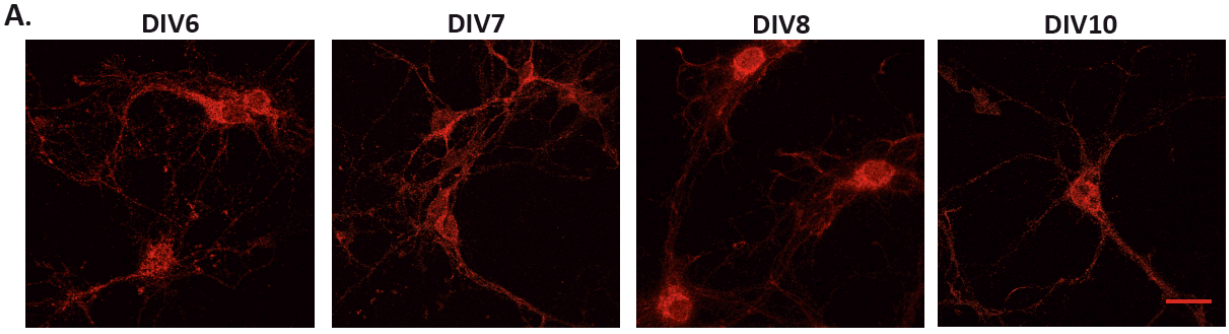
A.
DIV6
DIV7
DIV8
DIV10

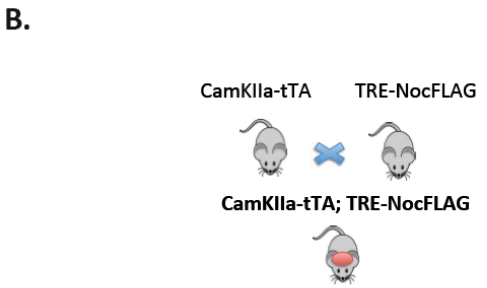
B.
CamKIIa-tTA
TRE-NocFLAG
CamKIIa-tTA; TRE-NocFLAG

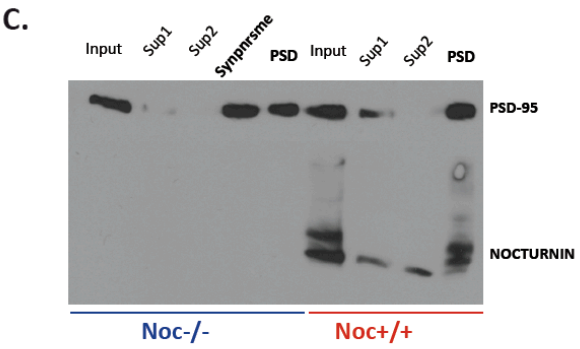
C.
Input
Sup1
Sup2
Synprsme
PSD
Input
Sup1
Sup2
PSD
PSD-95
NOCTURNIN
Noc-/-
Noc+/+

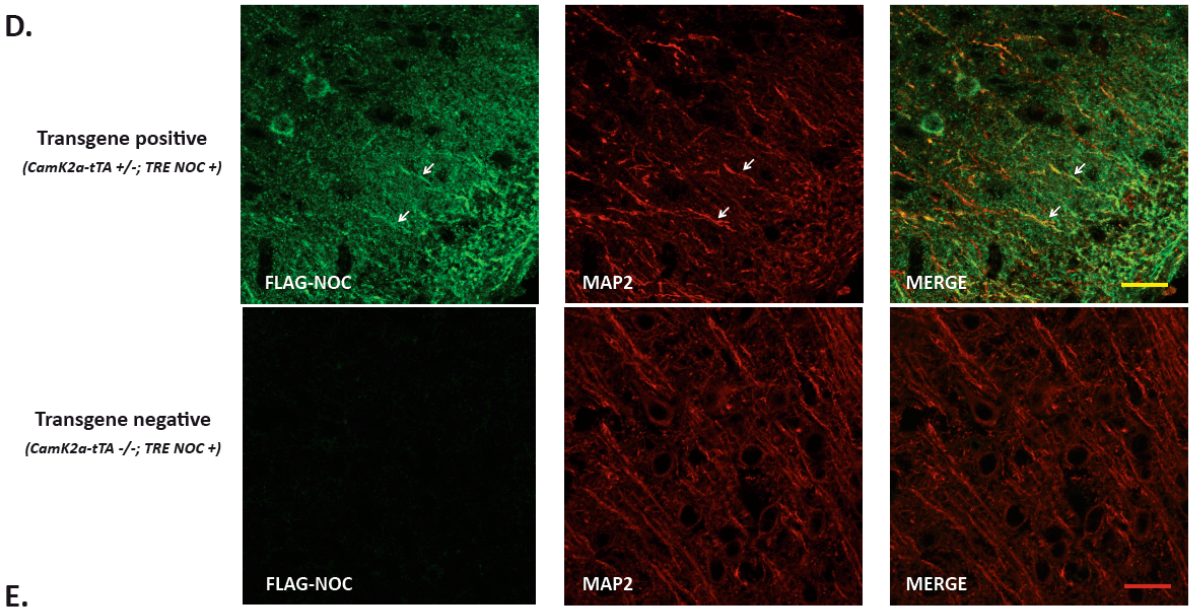
D.
Transgene positive
(CamK2a-tTA +/-; TRE NOC +)
FLAG-NOC
MAP2
MERGE
Transgene negative
(CamK2a-tTA -/-; TRE NOC +)
FLAG-NOC
MAP2
MERGE

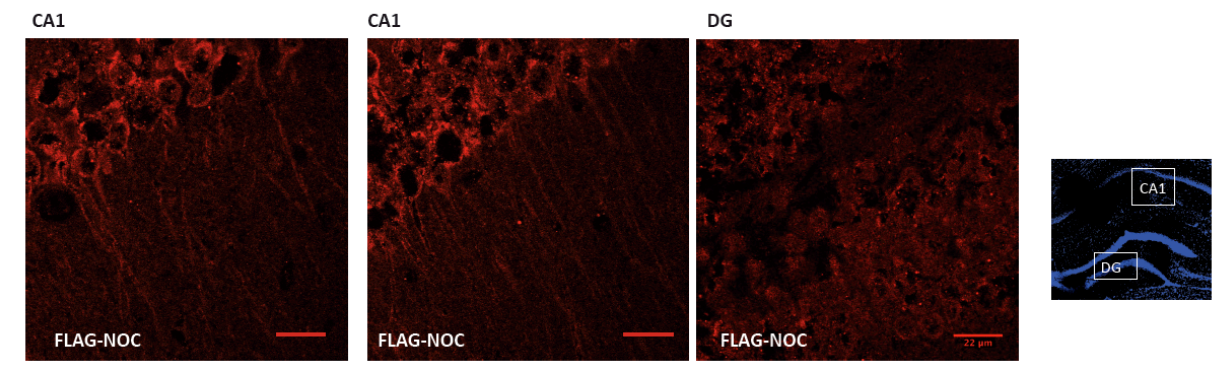
E.
CA1
CA1
DG
FLAG-NOC
FLAG-NOC
FLAG-NOC
CA1
DG

Figure 2. Comparison of hippocampal mGluR-induced LTD in *Noc-/-* and WT mice

(A) Schematic outline of the experimental setup. Extracellular field potentials (FPs) were measured in the stratum radiatum region of CA1 neurons elicited by Schaffer collateral stimulation. (B) LTD measurements from the first cohort of *Noc-/-* and WT mice. *Insets* show representative fEPSPs, pre and posttreatment. mGluR-LTD was induced by bath application of mGluR1/5 agonist (*RS*)-3,5-DHPG (100 μM, 5min). The fEPSP slope is plotted as the percent of pre-DHPG baseline. Synaptic strength was measured as the initial slope (10–40% of the rising phase) of the FP. LTD magnitude was compared at 50–60 min after the onset of DHPG. Graph on the right shows the comparison of the last 10 minute averages of LTD (50-60 min after the onset of DHPG) from *Noc-/-* mice and WT littermates. Euthasol was used as anesthetic in this cohort. N=12-14 slices from 7-11 mice. DHPG, (RS)-3,5-dihydroxyphenylglycine. (C) LTD measurements form the second cohort of mice. Ketamine was used as anesthetic in the second cohort. N= 25, 20.

***$p<0.001$ as analyzed by two-tailed Student's t-test. Data are represented as mean ± s.e.m.

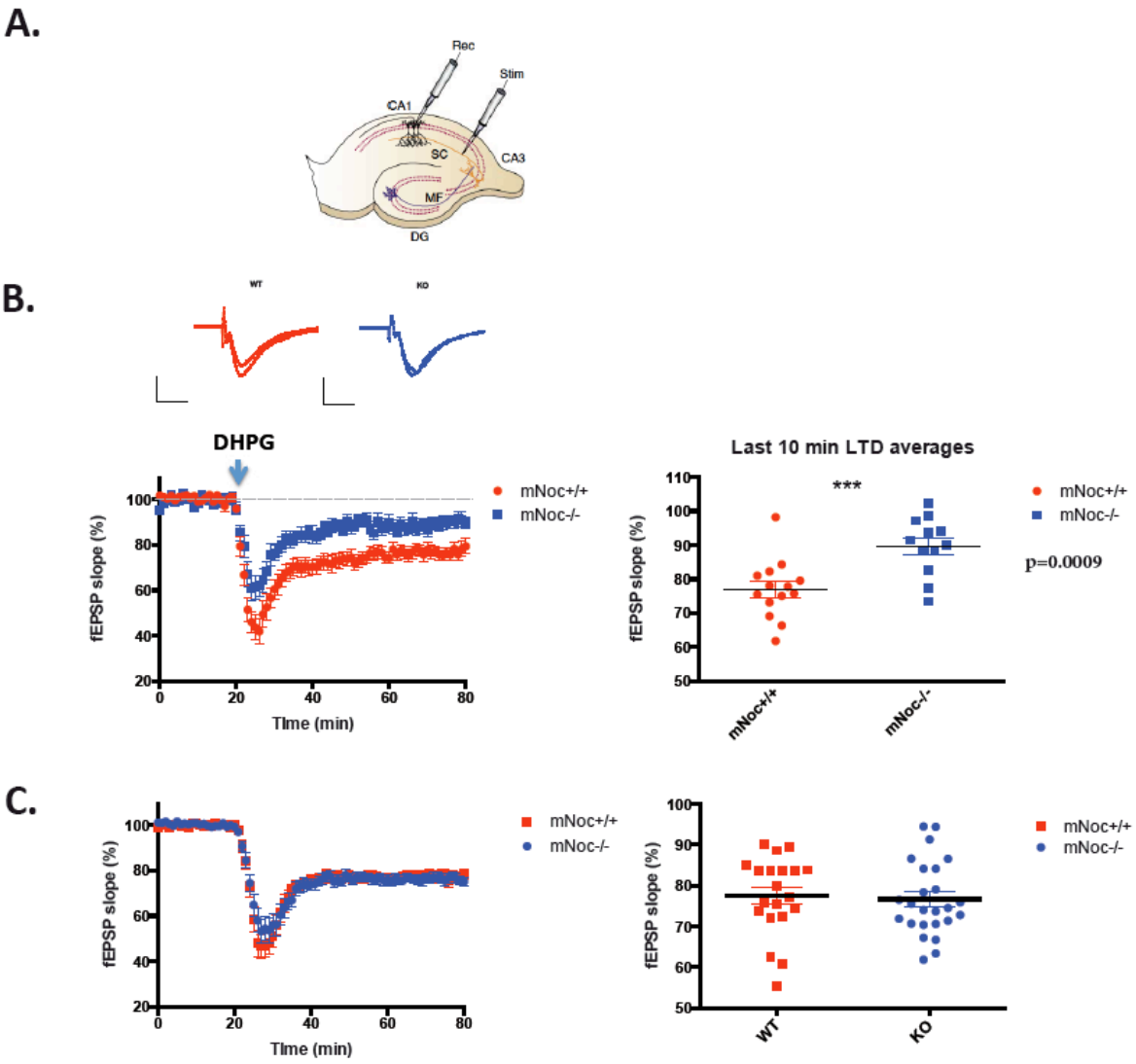
A.
Rec
Stim
CA1
SC
CA3
MF
DG
B.
WT
KO
DHPG
fEPSP slope (%)
Time (min)
mNoc+/+
mNoc-/-
Last 10 min LTD averages
***
p=0.0009
C.
WT
KO

Figure 3. Basal synaptic transmission is not altered in *Noc-/-* mice

(A) Input-output curves were plotted for *Noc-/-* mice and WT littermates. N=7-9 slices per genotype. Effect of genotype N.S., p=0.83. (B) Graph showing paired-pulse facilitation in *Noc-/-* and WT mice. fEPSPslope2/fEPSPslope1 is plotted as a function of interstimulus interval. N=18-19 slices per genotype. Effect of genotype N.S, p=0.0878.

N.S., non-significant, as analyzed by two-way ANOVA. Data are represented as mean ± s.e.m.

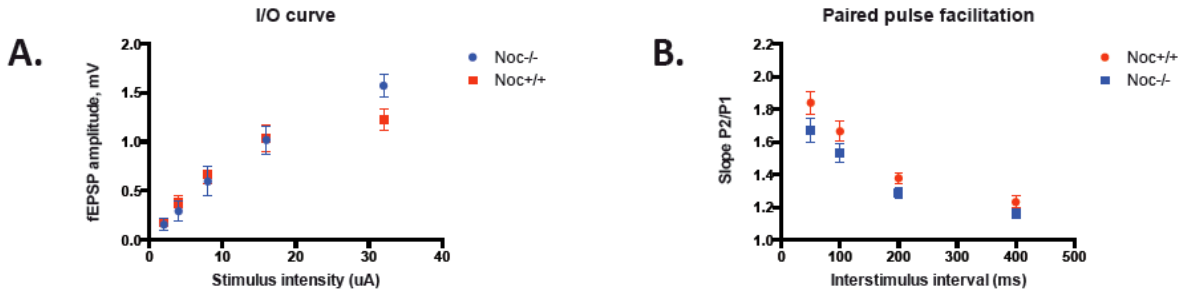
A.
I/O curve
fEPSP amplitude, mV
Stimulus intensity (uA)
Noc-/-
Noc+/+
B.
Paired pulse facilitation
Slope P2/P1
Interstimulus interval (ms)
Noc+/+
Noc-/-

Discussion

In this study I report that Nocturnin is present in the dendrites and in post-synaptic density in neurons which suggests that Nocturnin might have a functional role in the synapse. We initially observed a significant impairment when we measured mGluR-LTD in *Noc-/-* mice but we were not able to replicate this in an independent cohort. I used male and female mice for the LTD measurements and thought gender could be one potential source of variability. However, I didn't observe any significant differences between genders.

One methodical difference between the two cohorts was the use of different anesthetics. Thus, I used Euthasol as anesthetic in the first cohort of mice and I switched to Ketamine/Xylazine as anesthetic in the second cohort, due to a decline in slice health which significantly improved with the switch from Euthasol to Ketamine/Xylazine. The differences in the mechanism of action of these two anesthetics could have contributed to the inconsistency. Thus, Euthasol is a pentobarbital based anesthetic which acts on GABA receptors and depresses the nervous system by enhanced GABA activity. Ketamine, one the other hand, is an NMDA agonist which becomes an NMDA antagonist at high doses. It also has direct effects on dopaminergic and seratonergic receptors. One recent study examined how different anesthetics effect the metabolome and found profound alterations in metabolite levels between tissues where different anesthetics were used prior to tissue collection (Overmyer et al., 2015). We know that Nocturnin is an immediate early gene that is acutely induced in response to a number of different stimuli. In the previous chapter we reported a robust accumulation of succinate in BAT tissue of *Noc-/-* mice in response to a prolonged

cold exposure (Figure 5). Succinate is considered to be an indication of ROS activation and oxidative stress. It is possible that slices prepared with Euthasol were in a more depressed state and *Noc*-/- mice were more susceptible for ROS accumulation than WT mice as they might be lacking some antioxidant mechanisms due to metabolic alterations that were discussed in previous chapters. ROS accumulation is one of the hallmarks of neurodegenerative diseases and is associated to impairments in synaptic plasticity (Beckhauser et al., 2016). Thus, ROS accumulation in *Noc*-/- might be the reason for the impaired mGLuR-LTD in the first cohort. More studies are needed to elucidate Nocturnin's synaptic function.

Methods

Electrophysiology

Acute hippocampal brain slices were prepared from 28- 35 days old mice. Briefly, mice were anesthetized with ketamine (120 mg/kg)/xylazine (16 mg/kg) and transcardially perfused with chilled (4°C) sucrose dissection buffer containing the following (in mM): 2.6 KCl, 1.25 NaH_2PO_4, 26 $NaHCO_3$, 0.5 $CaCl_2$, 5 $MgCl_2$, 212 sucrose, and 10 dextrose aerated with 95% O_2/5% CO_2. Transverse hippocampal slices were obtained on a Leica VT1200S slicer. CA3 was cut off to avoid epileptogenic activity induced by DHPG. Slices recovered at and were maintained at 30°C in ACSF for 3 hrs. For all recordings, slices were submerged and perfused with ACSF contained the following (in mM): 119 NaCl, 2.5 KCl, 2 CaCl2, 1 MgCl2, 26 NaHCO3, 1 NaH_2PO_4 and 11 D-glucose aerated with 95% O_2/5% CO_2 to pH 7.4. Flow rate was set at 2.5–3.5 ml/min (30 ± 1°C). Field potentials (FPs) and EPSCs were evoked by stimulation of the Schaffer collateral pathway with a concentric bipolar tungsten electrode. Field potentials were recorded with a glass electrode (1 MΩ) filled with ACSF placed in the stratum radiatum of CA1. Test stimuli were delivered every 30 s and a stable baseline was obtained at ~50% of the maximum FP amplitude. The initial slope of the FP was used to measure stability of synaptic responses and quantify the magnitude of LTD. LTD was elicited by application of 50 μM DHPG for 5 min.

Neuronal cultures

Primary cortical neuronal cultures were prepared from E16 embryos. Briefly, cortex from embryos were dissected under a dissecting microscope and cut into 2-3 pieces in a 35 mm dish. Next, samples were washed in 1X pre-warmed dissection media. Samples were then trypsinized (final concentration 0.25%) and incubated for 20 min in 37°C CO_2 incubator. 15ml of plating media (Advanced DMEM, Life Technologies 12491-023; 10%FBS; 1X Glutamax, Life Technologies 35050-061) was added into trypsinized cortex tissues. Cells were filtered using a cell strainer and centrifuged at 2000rpm for 4 min at RT. Supernatant was discarded and cells were resuspended in plating media. Cells were seeded on coverslips at desired density and maintained in Neurobasal medium supplemented with 1X B27 and 1X Glutamax.

Immunofluorescence

For neuronal cultures, cells were fixed between DIV6-10 with 4%PFA and standard immunofluorescence protocol was used for staining with different antibodies. For brain slices, mice were transcardially perfused with 4% PFA and brain tissue was cryopreserved by 30%sucrose/PBS at 4°C for couple days. Tissue was then cryofrozen in OCT compound (Tissue Tek) on dry ice and kept at -80°C until sectioning. Brains were coronally sectioned using a cryostat at -20°C. Tissues were embedded on coverslips and processed for immunofluorescence.

CHAPTER FOUR

CONCLUSIONS AND FUTURE DIRECTIONS

Dual-localization of Nocturnin and its regulation

Our results, in combination with previous studies, indicate a tissue-specific, multi-functional role for Nocturnin. Despite the evidence suggesting its role as a deadenylase in vitro, my work as well as work from others have shown that in certain instances Nocturnin can lead to stabilization of transcripts (Green et al., 2007; Niu et al., 2011). Our results also indicate that Nocturnin has dual localization in the cytoplasm and mitochondria, which suggests a multi-functional role for Nocturnin based on its location and interaction with compartment-specific partners and targets. One awaiting question is the relative distribution of cytoplasmic vs. mitochondrial Nocturnin in different tissues and if these ratios change in response to stimulation like cold response. Based on biochemical fractionation from BAT tissue, I observed comparable levels of Nocturnin in mitochondrial and cytoplasmic fractions at RT. One remaining question is whether the mitochondrial:cytoplasmic Nocturnin ratio changes upon cold exposure and if these changes coincide with Nocturnin's role in cold-adaptive mechanisms. To test for the contribution of cytoplasmic vs. mitochondrial Nocturnin specifically into these cold-adaptive mechanisms described in the previous chapter, we can generate M1A and M65A mutants in brown adipocytes, enforcing translation initiation at the first or second AUG to generate mitochondrial or cytoplasmic Nocturnin. We

can then observe if localization of Nocturnin in either mitochondria or cytoplasm is sufficient to rescue the mitochondrial impairment. We can also use β-adrenergic agonists to stimulate cold-induced pathways in these cells and perform live imaging to visualize Nocturnin localization.

If mitochondrial:cytoplasmic Nocturnin ratio changes upon cold exposure, what are the mechanisms dictating cold-induced localization of Nocturnin? One potential mechanism is alternative regulation of translation via leaky scanning mechanism upon cold. This kind of translational regulation upon cellular stresses like hypoxia or nutrient deprivation has been previously shown (Barbosa et al., 2013; Dey et al., 2010). For example, gene encoding activating transcription factor 4 (ATF4) is regulated at the level of translation by two upstream open reading frames (uORFs) such that translation of the main ORF is favored upon cellular stress situations (Barbosa et al., 2013). To determine if the ratio of alternative start codon usage for the translation of Nocturnin changes upon cold, we can perform global translation initiation sequencing (GTI-seq) as previously described (Lee et al., 2012) and compare ribosomal occupancy of the alternative translation initiation codons in BAT from mice kept in cold or RT conditions. Briefly, this method uses both Cycloheximide (CHX) and Lactimidomycin (LTM) as ribosome E-site translation inhibitors. CHX binds to all translating ribosomes whereas LTM preferentially binds to initiating ribosomes and this allows us to distinguish between translation initiation and elongation.

Another mechanism dictating mitochondrial localization of Nocturnin upon cold could be alterations in mitochondrial import efficiency. Thus, it has been shown that mitochondrial stress response can alter localization (and function) of activating transcription

factor associated with stress-1 (ATFS-1) by altering its mitochondrial import efficiency (Nargund et al., 2012). To test if mitochondrial import efficiency is altered for Nocturnin in response to cold, we can perform in vitro mitochondrial import assay as previously described (Bihlmaier et al., 2008). Briefly, radiolabeled precursor Nocturnin will be incubated with isolated mitochondria from cold-exposed BAT and RT BAT in a mitochondrial import buffer. We can perform this experiment in the presence or absence of mitochondrial membrane potential in order to determine if the import is membrane potential dependent. In order to test if mitochondrial import is altered in vivo in response to cold, we can immunoprecipitate Nocturnin at cold and RT conditions from cytoplasmic and mitochondrial fractions of BAT and perform N-terminal sequencing of the peptide. This experiment will give us information on the abundance of: 1) Nocturnin without N-terminal MTS sequence (cytoplasmic) 2) Nocturnin that has N-terminal MTS that has not been transported into the mitochondria 3) Nocturnin within mitochondria without MTS, as its MTS gets cleaved once within the mitochondria (mitochondrial). We can also measure mitochondrial membrane potential in BAT from cold-exposed and RT mice using fluorescence-based methods like flow-cytometry. Determining the ratios of cytoplasmic vs. mitochondrial Nocturnin in BAT and in different tissues upon stimuli known to induce Nocturnin would give us a better insight on the mechanism of Nocturnin's tissue and condition-specific roles.

Mechanisms underlying Nocturnin's role in the mitochondria

In chapter 2, I showed that the stability of the mitochondrial-encoded transcripts is impaired in the BAT from *Noc-/-* mice upon an acute cold-exposure. This result was surprising, as it is the opposite of what we would expect if Nocturnin were to act as a deadenylase. It should be mentioned, however, that how polyadenylation/deadenylation works in the context of mitochondrial-encoded transcripts is not clear. Thus, knockdown and overexpression studies targeting mitochondrial poly(A) polymerase (MTPAP) and a mitochondrial deadenylase; phosphodiesterase 12 (PDE12) resulted in conflicting results where some mitochondrial-encoded transcripts were stabilized and some were destabilized (Rorbach and Minczuk, 2012; Rorbach et al., 2011; Slomovic et al., 2005; Tomecki et al., 2004; Wydro et al., 2010). Interestingly, in bacteria, polyadenylation stimulates RNA degradation (Rorbach and Minczuk, 2012). Considering the prokaryotic ancestry of mitochondria, Slomovic et al. suggested that stabilizing and destabilizing polyadenylation coexist in mitochondria (Slomovic et al., 2005).

Previous studies have shown that Nocturnin's deadenylase function is not as robust when compared to other deadenylases like PARN (Garbarino-Pico et al., 2007). One possibility is that Nocturnin binds to mitochondrial mRNAs and prevents binding of other more active deadenylases as well as poly(A) polymerases, thereby promoting stability by protecting transcripts from deadenylation and further adenylation. In our study, *Noc-/-* mitochondrial transcripts from *Noc -/-* BAT exhibited a trend toward higher expression than WT at RT, followed by a loss of stability upon cold exposure. This increase of transcript

levels in *Noc-/-* BAT at RT suggests that Nocturnin could be acting as a buffer in response to challenge conditions like cold exposure by post-transcriptionally regulating the mitochondrial transcript levels such that they will be prevented from steep changes. The levels of the stabilizing and destabilizing factors (like MTPAP and PDE12) could be disproportionate at RT and cold conditions and result in a discrepancy of transcript levels at RT and cold in *Noc-/-*. It should also be noted that I performed control experiments at RT (20-25°C) which is sub-thermoneutral for mice. Thus, BAT in these mice would be slightly activated. The increase in transcript levels of *Noc-/-* BAT at RT could also be due to compensatory changes in the system in response to the mitochondrial deficit- possibly by activating certain signaling cascades via systemic stress signals like ROS.

Another possibility is that Nocturnin interacts with stabilizing factors like MTPAP and LRPPRC. Thus, Nocturnin could be physically interacting with MTPAP and LRPPRC to form a complex that help maintain mitochondrial transcript stability. Indeed, previous mass-spectrometry and immunoprecipitation studies in our lab showed an interaction between Nocturnin and LRPPRC (unpublished data). In order to test Nocturnin's potential interactions with MTPAP and LRPPRC, immunoprecipitation at RT and cold conditions could be utilized. Knockdown or CRISPR techniques could be used to modify the expression of these genes followed by the analysis of mitochondrial gene expression as well as functional assays of mitochondria. Lentiviral approaches could be used to target Nocturnin to the mitochondria and to the cytoplasm exclusively and to observe if the mitochondrial or the cytoplasmic Nocturnin alone would be sufficient to rescue the mitochondrial phenotypes (Figures 2-2 and 2-4) in the absence/presence of MTPAP and LRPPRC. Additionally, we might be able to use

CRISPR or shRNA in order to knockout or knockdown endogenous mitochondrial *Nocturnin* specifically.

Lastly, Nocturnin might intervene with mitochondrial transcriptional machinery directly. We observed a loss of stability in almost all mt-mRNAs, including mt-ND6, which does not have a poly(A) tail, suggesting the effect of Nocturnin on mt-RNA stability could be independent of poly(A) tail length regulation (Figure 2-4B). The regulation of transcription and translation of mt-DNA is multilayered and intertwined, such that an impairment at any of the components might lead to a global reduction of mt-RNA expression(Hallberg and Larsson, 2014). For instance, according to tRNA punctuation model, mt-tRNAs serve as flanking regions of the mitochondrial primary transcripts, and endonucleolytic cleavages occur immediately before or after these tRNA sequences (Ojala et al., 1981). In Drosophila, it has been shown that polyadenylation is important for the maturation of specific tRNAs (Bratic et al., 2016). Nocturnin could be interacting with tRNAs and helping with recognition of proper cleavage sites in primary transcripts. CLIP-seq or RNA immunoprecipitation studies from mitochondrial fraction of BAT would help determine Nocturnin's mt-RNA targets in the mitochondria. We can also utilize brown adipocytes and perform CLIP-seq or RNA immunoprecipitation upon stimulation of these cells by β-adrenergic agonists in order to mimic BAT activation and determine Nocturnin's mt-RNA targets upon stimulation.

Regulation of glycosylation by Nocturnin

Based on my RNA-seq results, glycosylation enzymes in WT BAT were uniquely downregulated in response to cold-exposure as compared with *Noc-/-* BAT. I also previously mentioned the circadian component of BAT thermogenesis, and that the thermogenesis gene *Ucp1* is rhythmic and can be repressed upon cold exposure by REV-ERBα. It would be interesting to see if glycosylation is under circadian control and if it contributes to circadian regulation of thermogenesis via Nocturnin. Although we know that *Nocturnin* peaks at night when mice are active under normal conditions, it needs to be assessed if *Nocturnin* is still circadian upon prolonged cold exposure. For instance, under high fat diet, which is another condition to induce *Nocturnin* acutely, *Nocturnin* maintains its circadian rhythm but has an increased amplitude of night-time peak (Stubblefield et al., 2018). If similar is true under prolonged cold exposure, we would expect Nocturnin to maximize the thermogenic capacity of mice at night, with concomitant decreases in glycosylation. Proteomics analysis from tissue collected at different times of the day in WT and *Noc-/-* mice will help us understand if glycosylation is rhythmic globally in WT. *O*-GlcNAc glycosylation can be measured quantitatively by mass spectrometry-based proteomics combined with chemoenzymatic tagging of *O*-GlcNAc proteins (Khidekel et al., 2007). We could also focus on some potential targets that are already known to be glycosylated upon cold. One potential candidate is Phosphofructokinase-1 (PFK1), which is the enzyme that converts Fructose-6-phoshate to Fructose 1,6-biphosphate. In a recent paper it was shown that PFK1 glycosylation is a key regulator of the metabolic alterations necessary for cancer cell growth (Yi et al., 2012). Thus,

glycosylation inhibits PFK1 activity and diverts the glucose to pentose phosphate pathway in this particular example of cancer cells. Another example of cold-induced glycosylation is angiopoietin-like 4 (ANGPTL4), which is inhibited upon glycosylation upon sustained cold which leads to repartitioning of lipid fuel (Dijk et al., 2015). Glycosylation of these known targets could be assessed in WT and *Noc-/-* mice upon cold exposure by immunoblotting using an anti- *O*-GlcNAc antibody as previously shown (Yi et al., 2012).

Metabolic alterations in *Noc-/-* brown adipose tissue

Interestingly, I observed striking metabolic alterations in BAT from *Noc-/-* mice, in response to a prolonged cold exposure but not to an acute cold exposure protocol (Figure 6A and 6B). Yet, I observed a deficiency in thermogenic recovery in the *Noc-/-* mice after a relatively short exposure to cold (8-12 hrs) (Figure 2-3C), but longer term cold adaptive mechanisms seemed intact in *Noc-/-* (data not shown). It is likely that compensatory mechanisms are active in *Noc-/-* BAT which contribute to maintaining core body temperature. One possible explanation is that there is increased beiging of WAT in *Noc-/-* mice (compared with wildtype mice) which compensates for temperature recovery in response to prolonged cold exposure. Analysis of browning of WAT in *Noc-/-* and WT mice in RT and cold conditions by measuring levels of mitochondrial content and beigeing markers like *Ucp1* in subcutaneous inguinal WAT tissue would help assess this compensation.

In order to decipher the mechanisms of the metabolic alterations in *Noc-/-* mice upon cold, the fate of glucose in *Noc-/-* and WT mice can be determined by isotopical glucose labeling as previously described (Buescher et al., 2015; Mullen et al., 2014). Briefly, ^{13}C-labeled glucose will be injected to *Noc-/-* and WT mice and the fate of glucose will be assessed at RT and cold conditions by measuring the ^{13}C pool in TCA cycle metabolites like citrate in the mitochondria. If Nocturnin acts as a switch to divert glucose to the mitochondria upon cold exposure, as discussed in the previous chapter (Figure 2-9), we expect to see less ^{13}C from glucose when we measure citrate in the *Noc-/-* mitochondria. Additionally, we can perform cell-based assays using brown adipocytes to gain further mechanistic insight on how the metabolic pathways are altered in the *Noc-/-* BAT. We can silence key enzymes of the TCA cycle using RNAi or lentiviral-mediated shRNAs targeting the enzyme of interest concomitant with isotope labeling experiments to help decipher the specific pathways and enzymes contributing to the increase in TCA cycle metabolites in *Noc-/-*. In order to measure the contribution of glycosylation to glucose utilization, we can perform similar isotope labeling experiments together with pharmacological manipulation of glycosylation. This can be achieved by overexpression of *O*-GlcNAc transferase or pharmacological inhibition of **β**-N–acetylglucosaminidase (the glycosidase that removes *O*-GlcNAc) in order to increase global glycosylation.

Lastly, we observed almost 10-fold increase in succinate levels in *Noc-/-* upon prolonged cold exposure. As previously discussed, succinate accumulation is consistent with a mitochondrial deficit and it is also implicated in conditions like hypoxia or ischemia where the system is redirected towards anaerobic metabolic pathways for generating substrates

(Chouchani et al., 2014; Weinberg et al., 2000). This succinate pool in *Noc-/-* mice might be accumulated from oxidation of glutamine as there is an increase in glutamate in *Noc-/-* BAT. Interestingly, Pfas, which converts glutamine to glutamate is uniquely downregulated in WT in response to cold, as well as Slc25a22, which is involved in transport of glutamate across IMM. To examine the contribution of glutamine to TCA cycle metabolites in *Noc-/-* and WT mice we can perform isotope labeling by ^{13}C-labeled glutamine.

Succinate accumulation is also closely related to ROS production. Although higher levels of ROS is thought to be detrimental to the cell, small amounts of ROS can be beneficial as it initiates signaling cascades which could have beneficial effects for the organism. Interestingly, one recent paper reported overall systemic benefits in mice like protection from obesity and hepatic steatosis upon a high-fat diet that are secondary to mitochondrial dysfunction in BAT (Masand et al., 2018). They suggested these systemic benefits could be due to ROS signaling to the nucleus and possibly increasing transcription of humoral/systemic cues like Fgf21. Based on our findings which is consistent with this idea, it would be tempting to speculate that the systemic metabolic benefits in the *Noc-/-* mice like the lean phenotype, insulin sensitivity and protection from hepatic steatosis upon high-fat diet (Green et al., 2007) are all secondary to the mitochondrial deficit and increased ROS signaling. It should be noted that although increased ROS could be attributed to mitochondrial dysfunction, another mechanism underlying ROS could be inadequate detoxification. To determine if there is an increase in ROS levels in *Noc-/-* mice, measurements can be performed in vivo or ex vivo in tissue sections or in cultured cells from *Noc-/-* and WT mice using fluorescent dyes probing for ROS (Wang et al., 2013).

Additionally, making conditional knockout mice that lacks *Nocturnin* specifically in the BAT will give us a better mechanistic insight on the contribution of BAT to the systemic effects in *Noc*-/-mice.

APPENDIX A

BEHAVIORAL ANALYSIS OF NOC-/- MICE

A1. Analysis of cocaine sensitivity and anxiety in *Noc-/-* mice

Several studies connect drug-related behavior to circadian regulation. The interaction between drug response and components of central clock has been well studied. Mice that lack *mPer1* and *mPer2* both showed altered response to cocaine, *mPer1* knockout mice had little to no sensitization to cocaine, whereas *mPer2* knockout mice showed hypersensitization in response to cocaine (McClung et al., 2005). *Clock* mutant mice are reported to have increased levels of cocaine-induced locomotor sensitization as well as increased tyrosine hydroxylase expression in the ventral tegmental area (VTA) and increased dopaminergic cell firing in the VTA (McClung et al., 2005), which indicates CLOCK is involved in regulating the dopaminergic transmission in the reward circuitry of the brain. Since Nocturnin is partially regulated by the CLOCK, and since it is a circadian gene that is rhythmically expressed, at least in the periphery, we wanted to investigate whether Nocturnin knockout mice have any alterations in a psychostimulant response paradigm.

Cocaine-induced locomotor sensitization is thought to be an early indicator of the propensity for addiction. In order to investigate if the *Noc-/-* mice have an alteration in cocaine-evoked synaptic plasticity, we tested *Noc-/-* mice and their WT littermates in a two-injection cocaine-induced locomotor response test. Two-injection protocol has been

shown to be sufficient to cause locomotor sensitization to cocaine (Valjent et al., 2010). There was no difference between the responses of the genotypes in the first week of testing, yet interestingly, *Noc-/-* mice showed higher response to cocaine compared to WT littermates in the second week, after the second injection of cocaine (Figure A1). This is particularly interesting since it suggests an increased responsiveness to cocaine's longer-term effects in the *Noc-/-* mice, which could hint to enhanced cocaine-induced plasticity in the *Noc-/-* mice.

We also analyzed open-field behavior which measures exploratory behavior in mice and which is thought to be linked to anxiety-like behavior (Prut and Belzung, 2003) and found no differences between the genotypes.

Figure A1. *Noc-/-* mice have increased response to a repeated cocaine injection.

(A) Summary of experimental scheme. After 30 mins of baseline locomotor activity measurement, mice were injected by 20mg/kg cocaine and cocaine response was measured as velocity(mm/min) for the following 60 mins. Mice activity was tracked by a video-based system (LimeLight, Actimetrics). Representative traces of activity from individual mice are shown. For more details on method, see reference (Kumar et al., 2011). (B) Open field activity as measured during the 30 min baseline. Percent of time spent and distance traveled in different zones of test matrix corresponding center, periphery and corner are measured. (C) Cocaine response measurements from Noc-/- and WT mice. Upper graphs showing velocity as averaged every 5 mins after cocaine injection. Data analyzed by two-way repeated measures ANOVA, effect of genotype is insignificant for week 1 ($p=0.14$) but is significant for week 2 ($p<0.05$). Lower graphs showing average baseline, average of 30 min response after injection and net response, defined as baseline average subtracted from 30 min average response. N=9-11 per genotype.

All measurements were taken in two consecutive weeks.

*$p<0.05$ as analyzed by two-way repeated measures ANOVA or two-tailed Student's t-test.

Data are represented as mean ± s.e.m.

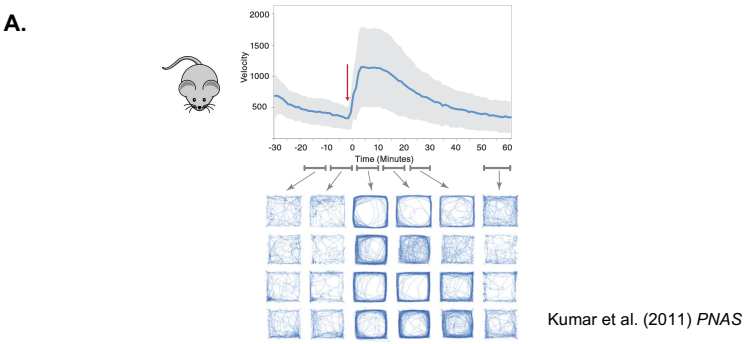
A.
Velocity
Time (Minutes)
Kumar et al. (2011) PNAS
B.
Week1
Week2
%Time Spent
%Distance traveled
Corner
Periphery
Center
Noc+/+
Noc-/-
C.
Velocity (mm/min)
Time (5min averages)
Baseline avg
30' avg
Resp-Baseline

A2. Analysis of learning and memory in Noc-/- mice

Fear conditioning is a well-established method to assess associative learning, where an unconditioned stimulus (US) such as foot shock is paired with a previously neutral cue such as tone, that becomes conditioned stimulus (CS) as a result of the associative learning. There are two types of fear conditioning; contextual and cue-dependent. Contextual fear conditioning is accepted to be a measure of hippocampal-dependent learning, although it is also dependent on the amygdala. Auditory cue fear conditioning, on the other hand, is mostly dependent on the lateral amygdala (Wehner and Radcliffe, 2004). Extinction is another form of learning, in which the animals learn that the conditioned stimulus (tone) is no longer associated with the conditioned fear response, in a context dependent manner. Anatomical correlates of extinction involve lateral and basolateral amygdala, as well as projections from the hippocampus and prefrontal cortex. We assessed Noc-/- mice in a 3-day extinction protocol and found no significant differences between Noc-/- and WT littermates (Figure A2).

Figure A2. Noc-/- mice have no alterations in extinction training or extinction retention from conditioned fear response

(A) Experimental scheme. For fear conditioning training, 4 CS-US (tone-shock) pairings were used. Different context and olfactory cue were used for extinction training and retention on Days 2&3. For extinction training, 20 10 sec tone (CS) presentations alone were given with 60 sec interstimulus intervals. For extinction retention, 15 10 sec tone (CS) presentations alone were given with 60 sec interstimulus intervals. (B) Percent freezing rates of Noc-/- and WT littermates on the day of fear conditioning training in response to 4 consecutive 80dB tone and 0.7mA shock pairings. (C) Graphs showing percent freezing in extinction from the conditioned fear response (left) and extinction retention (right). N=12-15 per genotype.

A.

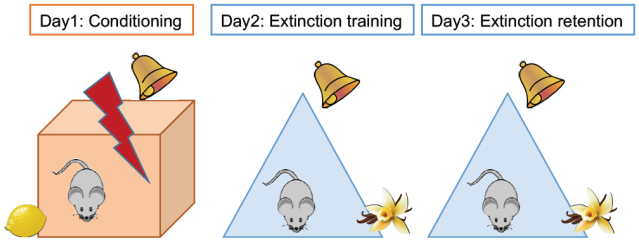
Day1: Conditioning
Day2: Extinction training
Day3: Extinction retention

B.

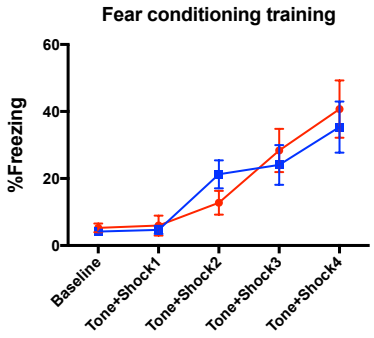
Fear conditioning training
%Freezing
60
40
20
0
Baseline
Tone+Shock1
Tone+Shock2
Tone+Shock3
Tone+Shock4

C.

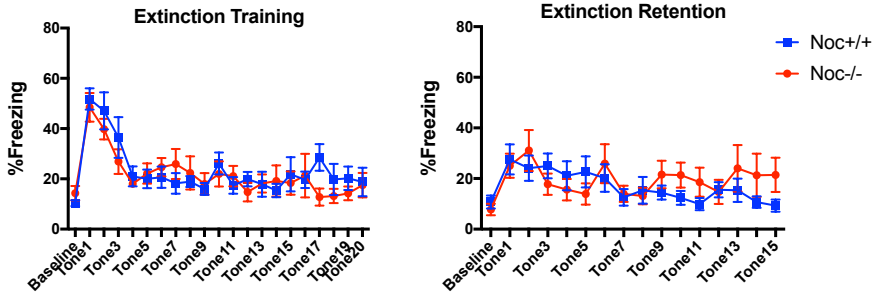
Extinction Training
Extinction Retention
%Freezing
80
60
40
20
0
Baseline
Tone1
Tone3
Tone5
Tone7
Tone9
Tone11
Tone13
Tone15
Tone17
Tone19
Tone20
Noc+/+
Noc-/-

APPENDIX B

B1. List of Primers

Oligo Number	Name	Sequence 5'-3'
2955	MT-ND1(Mouse), Forward	AATCGCCATAGCCTTCCTAA
2956	MT-ND1(Mouse), Reverse	GCGTCTGCAAATGGTTGTAA
2959	MT-ND2 (Mouse), Forward	CACAATATCCAGCACCAACC
2960	MT-ND2 (Mouse), Reverse	GAGGCTGTTGCTTGTGTGAC
2963	MT-CO1 (Mouse), Forward	GGTGGTCTAACCGGAATTGT
2964	MT-CO1 (Mouse), Reverse	GATAGCAAACACTGCTCCCA
2967	MT-CO2 (Mouse), Forward	GCCGACTAAATCAAGCAACA
2968	MT-CO2 (Mouse), Reverse	CAATGGGCATAAAGCTATGG
2971	MT-ATP8 (Mouse), Forward	GGCACCTTCACCAAAATCACT
2972	MT-ATP8 (Mouse), Reverse	TGGGGTAATGAATGAGGCAAAT
2973	MT-ATP6 (Mouse), Forward	CAGGCTTCCGACACAAACTA
2974	MT-ATP6 (Mouse), Reverse	TGTAAGCCGGACTGCTAATG
2977	MT-CO3 (Mouse), Forward	GCCCTCCTTCTAACATCAGG
2978	MT-CO3 (Mouse), Reverse	GCCTTGGTAGGTTCCTTCAC
2981	MT-ND3 (Mouse), Forward	AATGCGGATTCGACCCTA
2982	MT-ND3 (Mouse), Reverse	TGAATTGCTCATGGTAGTGGA
2985	MT-ND4L (Mouse), Forward	ACTCCAACTCCATAAGCTCCA
2986	MT-ND4L (Mouse), Reverse	TTTGGACGTAATCTGTTCCG
2989	MT-ND4 (Mouse), Forward	TATTACCCGATGAGGGAACC
2990	MT-ND4 (Mouse), Reverse	AGGGCAATTAGCAGTGGAAT
2993	MT-ND5 (Mouse), Forward	ACCCATGACTACCATCAGCA
2994	MT-ND5 (Mouse), Reverse	GGAATCGGACCAGTAGGAAA
2997	MT-ND6 (Mouse), Forward	AGCACAACTATATATTGCCGCTAC
2998	MT-ND6 (Mouse), Reverse	GATGGTTTGGGAGATTGGTT
3001	MT-CYTB (Mouse), Forward	CATTCTGAGGTGCCACAGTT
3002	MT-CYTB (Mouse), Reverse	GATGAAGTGGAAAGCGAAGA
3005	MT-RNR2 (Mouse), Forward	CCTAGGGATAACAGCGCAAT
3006	MT-RNR2 (Mouse), Reverse	ATCGTTGAACAAACGAACCA
3009	MT-RNR1 (Mouse), Forward	TGAGCAATGAAGTACGCACA
3010	MT-RNR1 (Mouse), Reverse	TTCCAAGCACACTTTCCAGT
3013	mtDNA whole (Mouse), Forward	CCTATCACCCTTGCCATCAT
3014	mtDNA whole (Mouse), Reverse	GAGGCTGTTGCTTGTGTGAC
3015	nDNA whole (Mouse), Forward	ATGGAAAGCCTGCCATCATG
3016	nDNA whole (Mouse), Reverse	TCCTTGTTGTTCAGCATCAC
616	Noct-Exon3 (Mouse), Forward	ACCAGCCAGACATACTGTGC

617	Noct-Exon3 (Mouse), Reverse	CTTGGGGAAAAACGTGCCT
3125	Ucp1 (Mouse), Forward	GGCCTCTACGACTCAGTCCA
3126	Ucp1 (Mouse), Reverse	TAAGCCGGCTGAGATCTTGT
3129	Pparg (Mouse), Forward	AGGCGAGGGCGATCTTGACAG
3130	Pparg (Mouse), Reverse	AATTCGGATGGCCACCTCTTTG
1870	Ppargc1a (Mouse), Forward	GAAGAGATAAAGTTGTTGGTTTGGC
1871	Ppargc1a (Mouse), Reverse	AGACAAATGTGCTTCGAAAAAGAA
3109	B2m (Mouse), Forward	CTCGGTGACCCTGGTCTTC
3110	B2m (Mouse), Reverse	TTGAGGGGTTTTCTGGATAGCA
3199	Dio2 (Mouse), Forward	CAGTGTGGTGCACGTCTCCAA TC
3200	Dio2 (Mouse), Reverse	TGAACCAAAGTTGACCACCAG

B2. List of antibodies used for immunofluorescence (IF) and western blotting (WB)

Name	Type	Company	Dilution
ANTI-FLAG M2	Mouse, monoclonal	Sigma (F1804)	1:500 (IF)
MT-CO1	Mouse, monoclonal	Invitrogen (459600)	1:2000 (WB)
ANTI-α-TUBULIN	Mouse, monoclonal	Sigma (T6199)	1:50000 (WB)
VDAC	Rabbit, monoclonal	Cell Signaling (D73D12)	1:4000 (WB)
MT-CO2	Rabbit, polyclonal	Proteintech (55070-1-AP)	1:5000 (WB)
ACTIN	Mouse, monoclonal	Millipore (MAB1501)	1:50000 (WB)

B3. Links to RNA-Seq and metabolomics data

RNA-Seq:

/Volumes/PromisePegasus/yasemin_data/scratch/03269/kilarugk/yasemin_coldexposure_KGK_dec2017_tacc/output/star_out/deg_with_chrM_noncoding_genes_RPKM_filtered/deseq2

Metabolomics:

/Volumes/PromisePegasus/yasemin_data/YO Metabolomics

BIBLIOGRAPHY

Akhtar, R.A., Reddy, A.B., Maywood, E.S., Clayton, J.D., King, V.M., Smith, A.G., Gant, T.W., Hastings, M.H., and Kyriacou, C.P. (2002). Circadian cycling of the mouse liver transcriptome, as revealed by cDNA microarray, is driven by the suprachiasmatic nucleus. Curr Biol *12*, 540-550.

Baggs, J.E., and Green, C.B. (2003). Nocturnin, a deadenylase in Xenopus laevis retina: a mechanism for posttranscriptional control of circadian-related mRNA. Curr Biol *13*, 189-198.

Barbosa, C., Peixeiro, I., and Romao, L. (2013). Gene expression regulation by upstream open reading frames and human disease. PLoS Genet *9*, e1003529.

Beckhauser, T.F., Francis-Oliveira, J., and De Pasquale, R. (2016). Reactive Oxygen Species: Physiological and Physiopathological Effects on Synaptic Plasticity. J Exp Neurosci *10*, 23-48.

Bihlmaier, K., Bien, M., and Herrmann, J.M. (2008). In vitro import of proteins into isolated mitochondria. Methods Mol Biol *457*, 85-94.

Bjorndal, B., Burri, L., Staalesen, V., Skorve, J., and Berge, R.K. (2011). Different adipose depots: their role in the development of metabolic syndrome and mitochondrial response to hypolipidemic agents. J Obes *2011*, 490650.

Bramham, C.R., and Wells, D.G. (2007). Dendritic mRNA: transport, translation and function. Nat Rev Neurosci *8*, 776-789.

Bratic, A., Clemente, P., Calvo-Garrido, J., Maffezzini, C., Felser, A., Wibom, R., Wedell, A., Freyer, C., and Wredenberg, A. (2016). Mitochondrial Polyadenylation Is a One-Step Process Required for mRNA Integrity and tRNA Maturation. PLoS Genet *12*, e1006028.

Brum, M.C., Filho, F.F., Schnorr, C.C., Bottega, G.B., and Rodrigues, T.C. (2015). Shift work and its association with metabolic disorders. Diabetol Metab Syndr *7*, 45.

Buescher, J.M., Antoniewicz, M.R., Boros, L.G., Burgess, S.C., Brunengraber, H., Clish, C.B., DeBerardinis, R.J., Feron, O., Frezza, C., Ghesquiere, B., et al. (2015). A roadmap for interpreting (13)C metabolite labeling patterns from cells. Curr Opin Biotechnol *34*, 189-201.

Cannon, B., and Nedergaard, J. (2004). Brown adipose tissue: function and physiological significance. Physiol Rev *84*, 277-359.

Cedikova, M., Kripnerova, M., Dvorakova, J., Pitule, P., Grundmanova, M., Babuska, V., Mullerova, D., and Kuncova, J. (2016). Mitochondria in White, Brown, and Beige Adipocytes. Stem Cells Int *2016*, 6067349.

Cela, O., Scrima, R., Pazienza, V., Merla, G., Benegiamo, G., Augello, B., Fugetto, S., Menga, M., Rubino, R., Fuhr, L., et al. (2016). Clock genes-dependent acetylation of complex I sets rhythmic activity of mitochondrial OxPhos. Biochimica et biophysica acta *1863*, 596-606.

Chinnery, P.F. (2015). Mitochondrial disease in adults: what's old and what's new? EMBO Mol Med *7*, 1503-1512.

Chouchani, E.T., Pell, V.R., Gaude, E., Aksentijevic, D., Sundier, S.Y., Robb, E.L., Logan, A., Nadtochiy, S.M., Ord, E.N.J., Smith, A.C., et al. (2014). Ischaemic accumulation of succinate controls reperfusion injury through mitochondrial ROS. Nature *515*, 431-435.

Cypess, A.M., Lehman, S., Williams, G., Tal, I., Rodman, D., Goldfine, A.B., Kuo, F.C., Palmer, E.L., Tseng, Y.H., Doria, A., et al. (2009). Identification and importance of brown adipose tissue in adult humans. N Engl J Med *360*, 1509-1517.

Cypess, A.M., Weiner, L.S., Roberts-Toler, C., Franquet Elia, E., Kessler, S.H., Kahn, P.A., English, J., Chatman, K., Trauger, S.A., Doria, A., et al. (2015). Activation of human brown adipose tissue by a beta3-adrenergic receptor agonist. Cell Metab *21*, 33-38.

Dey, S., Baird, T.D., Zhou, D., Palam, L.R., Spandau, D.F., and Wek, R.C. (2010). Both transcriptional regulation and translational control of ATF4 are central to the integrated stress response. J Biol Chem *285*, 33165-33174.

Dijk, W., Heine, M., Vergnes, L., Boon, M.R., Schaart, G., Hesselink, M.K., Reue, K., van Marken Lichtenbelt, W.D., Olivecrona, G., Rensen, P.C., et al. (2015). ANGPTL4 mediates shuttling of lipid fuel to brown adipose tissue during sustained cold exposure. Elife *4*.

Douris, N., Kojima, S., Pan, X., Lerch-Gaggl, A.F., Duong, S.Q., Hussain, M.M., and Green, C.B. (2011). Nocturnin regulates circadian trafficking of dietary lipid in intestinal enterocytes. Curr Biol *21*, 1347-1355.

Fedorenko, A., Lishko, P.V., and Kirichok, Y. (2012). Mechanism of fatty-acid-dependent UCP1 uncoupling in brown fat mitochondria. Cell *151*, 400-413.

Feldmann, H.M., Golozoubova, V., Cannon, B., and Nedergaard, J. (2009). UCP1 ablation induces obesity and abolishes diet-induced thermogenesis in mice exempt from thermal stress by living at thermoneutrality. Cell Metab *9*, 203-209.

Frezza, C., Cipolat, S., and Scorrano, L. (2007). Organelle isolation: functional mitochondria from mouse liver, muscle and cultured fibroblasts. Nat Protoc *2*, 287-295.

Gao, X., Wan, J., Liu, B., Ma, M., Shen, B., and Qian, S.B. (2015). Quantitative profiling of initiating ribosomes in vivo. Nat Methods *12*, 147-153.

Garbarino-Pico, E., Niu, S., Rollag, M.D., Strayer, C.A., Besharse, J.C., and Green, C.B. (2007). Immediate early response of the circadian polyA ribonuclease nocturnin to two extracellular stimuli. RNA *13*, 745-755.

Gerhart-Hines, Z., Feng, D., Emmett, M.J., Everett, L.J., Loro, E., Briggs, E.R., Bugge, A., Hou, C., Ferrara, C., Seale, P., et al. (2013). The nuclear receptor Rev-erbalpha controls circadian thermogenic plasticity. Nature *503*, 410-413.

Godwin, A.R., Kojima, S., Green, C.B., and Wilusz, J. (2013). Kiss your tail goodbye: the role of PARN, Nocturnin, and Angel deadenylases in mRNA biology. Biochimica et biophysica acta *1829*, 571-579.

Goh, B.C., Wu, X., Evans, A.E., Johnson, M.L., Hill, M.R., and Gimble, J.M. (2007). Food entrainment of circadian gene expression altered in PPARalpha-/- brown fat and heart. Biochem Biophys Res Commun *360*, 828-833.

Goldstrohm, A.C., and Wickens, M. (2008). Multifunctional deadenylase complexes diversify mRNA control. Nat Rev Mol Cell Biol *9*, 337-344.

Grechez-Cassiau, A., Panda, S., Lacoche, S., Teboul, M., Azmi, S., Laudet, V., Hogenesch, J.B., Taneja, R., and Delaunay, F. (2004). The transcriptional repressor STRA13 regulates a subset of peripheral circadian outputs. J Biol Chem *279*, 1141-1150.

Green, C.B., and Besharse, J.C. (1996). Identification of a novel vertebrate circadian clock-regulated gene encoding the protein nocturnin. Proceedings of the National Academy of Sciences of the United States of America *93*, 14884-14888.

Green, C.B., Douris, N., Kojima, S., Strayer, C.A., Fogerty, J., Lourim, D., Keller, S.R., and Besharse, J.C. (2007). Loss of Nocturnin, a circadian deadenylase, confers resistance to hepatic steatosis and diet-induced obesity. Proceedings of the National Academy of Sciences of the United States of America *104*, 9888-9893.

Green, C.B., Takahashi, J.S., and Bass, J. (2008). The meter of metabolism. Cell *134*, 728-742.

Hallberg, B.M., and Larsson, N.G. (2014). Making proteins in the powerhouse. Cell Metab *20*, 226-240.

Hammond, R.A., and Levine, R. (2010). The economic impact of obesity in the United States. Diabetes Metab Syndr Obes *3*, 285-295.

Harms, M., and Seale, P. (2013). Brown and beige fat: development, function and therapeutic potential. Nat Med *19*, 1252-1263.

Hatori, M., Vollmers, C., Zarrinpar, A., DiTacchio, L., Bushong, E.A., Gill, S., Leblanc, M., Chaix, A., Joens, M., Fitzpatrick, J.A., et al. (2012). Time-restricted feeding without reducing caloric intake prevents metabolic diseases in mice fed a high-fat diet. Cell Metab *15*, 848-860.

Hirschey, M.D., Shimazu, T., Goetzman, E., Jing, E., Schwer, B., Lombard, D.B., Grueter, C.A., Harris, C., Biddinger, S., Ilkayeva, O.R., et al. (2010). SIRT3 regulates mitochondrial fatty-acid oxidation by reversible enzyme deacetylation. Nature *464*, 121-125.

Holt, C.E., and Schuman, E.M. (2013). The central dogma decentralized: new perspectives on RNA function and local translation in neurons. Neuron *80*, 648-657.

Huber, K.M., Kayser, M.S., and Bear, M.F. (2000). Role for rapid dendritic protein synthesis in hippocampal mGluR-dependent long-term depression. Science *288*, 1254-1257.

Jang, C., Lahens, N.F., Hogenesch, J.B., and Sehgal, A. (2015). Ribosome profiling reveals an important role for translational control in circadian gene expression. Genome Res *25*, 1836-1847.

Janich, P., Arpat, A.B., Castelo-Szekely, V., Lopes, M., and Gatfield, D. (2015). Ribosome profiling reveals the rhythmic liver translatome and circadian clock regulation by upstream open reading frames. Genome Res *25*, 1848-1859.

Karlsson, B., Knutsson, A., & Lindahl, B. (2001). Is there an association between shift work and having a metabolic syndrome? Results from a population based study of 27 485 people. Occup. Environ. Med. *58*, 747-752.

Kawai, M., Delany, A.M., Green, C.B., Adamo, M.L., and Rosen, C.J. (2010a). Nocturnin suppresses igf1 expression in bone by targeting the 3' untranslated region of igf1 mRNA. Endocrinology *151*, 4861-4870.

Kawai, M., Green, C.B., Lecka-Czernik, B., Douris, N., Gilbert, M.R., Kojima, S., Ackert-Bicknell, C., Garg, N., Horowitz, M.C., Adamo, M.L., et al. (2010b). A circadian-regulated gene, Nocturnin, promotes adipogenesis by stimulating PPAR-gamma nuclear translocation. Proceedings of the National Academy of Sciences of the United States of America *107*, 10508-10513.

Khidekel, N., Ficarro, S.B., Clark, P.M., Bryan, M.C., Swaney, D.L., Rexach, J.E., Sun, Y.E., Coon, J.J., Peters, E.C., and Hsieh-Wilson, L.C. (2007). Probing the dynamics of O-GlcNAc glycosylation in the brain using quantitative proteomics. Nat Chem Biol *3*, 339-348.

Kim, J.H., and Richter, J.D. (2006). Opposing polymerase-deadenylase activities regulate cytoplasmic polyadenylation. Mol Cell *24*, 173-183.

Kochetov, A.V. (2008). Alternative translation start sites and hidden coding potential of eukaryotic mRNAs. Bioessays *30*, 683-691.

Koike, N., Yoo, S.H., Huang, H.C., Kumar, V., Lee, C., Kim, T.K., and Takahashi, J.S. (2012). Transcriptional architecture and chromatin landscape of the core circadian clock in mammals. Science *338*, 349-354.

Kojima, S., Gendreau, K.L., Sher-Chen, E.L., Gao, P., and Green, C.B. (2015). Changes in poly(A) tail length dynamics from the loss of the circadian deadenylase Nocturnin. Sci Rep *5*, 17059.

Kojima, S., Sher-Chen, E.L., and Green, C.B. (2012). Circadian control of mRNA polyadenylation dynamics regulates rhythmic protein expression. Genes Dev *26*, 2724-2736.

Kontani, Y., Wang, Y., Kimura, K., Inokuma, K.I., Saito, M., Suzuki-Miura, T., Wang, Z., Sato, Y., Mori, N., and Yamashita, H. (2005). UCP1 deficiency increases susceptibility to diet-induced obesity with age. Aging Cell *4*, 147-155.

Kozak, M. (2005). Regulation of translation via mRNA structure in prokaryotes and eukaryotes. Gene *361*, 13-37.

Krichevsky, A.M., and Kosik, K.S. (2001). Neuronal RNA granules: a link between RNA localization and stimulation-dependent translation. Neuron *32*, 683-696.

Kumar, V., Kim, K., Joseph, C., Thomas, L.C., Hong, H., and Takahashi, J.S. (2011). Second-generation high-throughput forward genetic screen in mice to isolate subtle behavioral mutants. Proceedings of the National Academy of Sciences of the United States of America *108 Suppl 3*, 15557-15564.

Lamia, K.A., Storch, K.F., and Weitz, C.J. (2008). Physiological significance of a peripheral tissue circadian clock. Proceedings of the National Academy of Sciences of the United States of America *105*, 15172-15177.

Lee, P., Bova, R., Schofield, L., Bryant, W., Dieckmann, W., Slattery, A., Govendir, M.A., Emmett, L., and Greenfield, J.R. (2016). Brown Adipose Tissue Exhibits a Glucose-Responsive Thermogenic Biorhythm in Humans. Cell Metab *23*, 602-609.

Lee, S., Liu, B., Lee, S., Huang, S.X., Shen, B., and Qian, S.B. (2012). Global mapping of translation initiation sites in mammalian cells at single-nucleotide resolution. Proceedings of the National Academy of Sciences of the United States of America *109*, E2424-2432.

Lein, E.S., Hawrylycz, M.J., Ao, N., Ayres, M., Bensinger, A., Bernard, A., Boe, A.F., Boguski, M.S., Brockway, K.S., Byrnes, E.J., et al. (2007). Genome-wide atlas of gene expression in the adult mouse brain. Nature *445*, 168-176.

Li, R., Yue, J., Zhang, Y., Zhou, L., Hao, W., Yuan, J., Qiang, B., Ding, J.M., Peng, X., and Cao, J.M. (2008). CLOCK/BMAL1 regulates human nocturnin transcription through binding to the E-box of nocturnin promoter. Molecular and cellular biochemistry *317*, 169-177.

Li, S., Yu, Q., Wang, G.X., and Lin, J.D. (2013). The biological clock is regulated by adrenergic signaling in brown fat but is dispensable for cold-induced thermogenesis. PloS one *8*, e70109.

Lim, C., and Allada, R. (2013). Emerging roles for post-transcriptional regulation in circadian clocks. Nat Neurosci *16*, 1544-1550.

Lowell, B.B., V, S.S., Hamann, A., Lawitts, J.A., Himms-Hagen, J., Boyer, B.B., Kozak, L.P., and Flier, J.S. (1993). Development of obesity in transgenic mice after genetic ablation of brown adipose tissue. Nature *366*, 740-742.

Marcheva, B., Ramsey, K.M., Buhr, E.D., Kobayashi, Y., Su, H., Ko, C.H., Ivanova, G., Omura, C., Mo, S., Vitaterna, M.H., et al. (2010). Disruption of the clock components CLOCK and BMAL1 leads to hypoinsulinaemia and diabetes. Nature *466*, 627-631.

Masand, R., Paulo, E., Wu, D., Wang, Y., Swaney, D.L., Jimenez-Morales, D., Krogan, N.J., and Wang, B. (2018). Proteome Imbalance of Mitochondrial Electron Transport Chain in Brown Adipocytes Leads to Metabolic Benefits. Cell Metab *27*, 616-629 e614.

Masri S, P.V., Eckel-Mahan KL, Peleg S, Forne I, Ladurner AG, Baldi P, Imhof A, Sassone-Corsi P (2013). Circadian acetylome reveals regulation of mitochondrial metabolic pathways. Proceedings of the National Academy of Sciences of the United States of America *110*, 3339-3344.

Mauvoisin, D., Wang, J., Jouffe, C., Martin, E., Atger, F., Waridel, P., Quadroni, M., Gachon, F., and Naef, F. (2014). Circadian clock-dependent and -independent rhythmic proteomes implement distinct diurnal functions in mouse liver. Proceedings of the National Academy of Sciences of the United States of America *111*, 167-172.

McClung, C.A., Sidiropoulou, K., Vitaterna, M., Takahashi, J.S., White, F.J., Cooper, D.C., and Nestler, E.J. (2005). Regulation of dopaminergic transmission and cocaine

reward by the Clock gene. Proceedings of the National Academy of Sciences of the United States of America *102*, 9377-9381.

Menet, J.S., Rodriguez, J., Abruzzi, K.C., and Rosbash, M. (2012). Nascent-Seq reveals novel features of mouse circadian transcriptional regulation. Elife *1*, e00011.

Michel, A.M., Fox, G., A, M.K., De Bo, C., O'Connor, P.B., Heaphy, S.M., Mullan, J.P., Donohue, C.A., Higgins, D.G., and Baranov, P.V. (2014). GWIPS-viz: development of a ribo-seq genome browser. Nucleic Acids Res *42*, D859-864.

Miller, B.H., McDearmon, E.L., Panda, S., Hayes, K.R., Zhang, J., Andrews, J.L., Antoch, M.P., Walker, J.R., Esser, K.A., Hogenesch, J.B., et al. (2007). Circadian and CLOCK-controlled regulation of the mouse transcriptome and cell proliferation. Proceedings of the National Academy of Sciences of the United States of America *104*, 3342-3347.

Mukherji, A., Kobiita, A., Damara, M., Misra, N., Meziane, H., Champy, M.F., and Chambon, P. (2015). Shifting eating to the circadian rest phase misaligns the peripheral clocks with the master SCN clock and leads to a metabolic syndrome. Proceedings of the National Academy of Sciences of the United States of America *112*, E6691-6698.

Mullen, A.R., Hu, Z., Shi, X., Jiang, L., Boroughs, L.K., Kovacs, Z., Boriack, R., Rakheja, D., Sullivan, L.B., Linehan, W.M., et al. (2014). Oxidation of alpha-ketoglutarate is required for reductive carboxylation in cancer cells with mitochondrial defects. Cell Rep *7*, 1679-1690.

Nagaike, T., Suzuki, T., Katoh, T., and Ueda, T. (2005). Human mitochondrial mRNAs are stabilized with polyadenylation regulated by mitochondria-specific poly(A) polymerase and polynucleotide phosphorylase. J Biol Chem *280*, 19721-19727.

Nagao, A., Hino-Shigi, N., and Suzuki, T. (2008). Measuring mRNA decay in human mitochondria. Methods Enzymol *447*, 489-499.

Nakahata, Y., Sahar, S., Astarita, G., Kaluzova, M., and Sassone-Corsi, P. (2009). Circadian control of the NAD+ salvage pathway by CLOCK-SIRT1. Science *324*, 654-657.

Nargund, A.M., Pellegrino, M.W., Fiorese, C.J., Baker, B.M., and Haynes, C.M. (2012). Mitochondrial import efficiency of ATFS-1 regulates mitochondrial UPR activation. Science *337*, 587-590.

Neufeld-Cohen, A., Robles, M.S., Aviram, R., Manella, G., Adamovich, Y., Ladeuix, B., Nir, D., Rousso-Noori, L., Kuperman, Y., Golik, M., et al. (2016). Circadian control of oscillations in mitochondrial rate-limiting enzymes and nutrient utilization by PERIOD

proteins. Proceedings of the National Academy of Sciences of the United States of America *113*, E1673-1682.

Niu, S., Shingle, D.L., Garbarino-Pico, E., Kojima, S., Gilbert, M., and Green, C.B. (2011). The circadian deadenylase Nocturnin is necessary for stabilization of the iNOS mRNA in mice. PloS one *6*, e26954.

O'Neill, J.S., van Ooijen, G., Dixon, L.E., Troein, C., Corellou, F., Bouget, F.Y., Reddy, A.B., and Millar, A.J. (2011). Circadian rhythms persist without transcription in a eukaryote. Nature *469*, 554-558.

Oishi, K., Atsumi, G., Sugiyama, S., Kodomari, I., Kasamatsu, M., Machida, K., and Ishida, N. (2006). Disrupted fat absorption attenuates obesity induced by a high-fat diet in Clock mutant mice. FEBS Lett *580*, 127-130.

Oishi, K., Miyazaki, K., Kadota, K., Kikuno, R., Nagase, T., Atsumi, G., Ohkura, N., Azama, T., Mesaki, M., Yukimasa, S., et al. (2003). Genome-wide expression analysis of mouse liver reveals CLOCK-regulated circadian output genes. J Biol Chem *278*, 41519-41527.

Ojala, D., Montoya, J., and Attardi, G. (1981). tRNA punctuation model of RNA processing in human mitochondria. Nature *290*, 470-474.

Orozco-Solis, R., Aguilar-Arnal, L., Murakami, M., Peruquetti, R., Ramadori, G., Coppari, R., and Sassone-Corsi, P. (2016). The Circadian Clock in the Ventromedial Hypothalamus Controls Cyclic Energy Expenditure. Cell Metab *23*, 467-478.

Overmyer, K.A., Thonusin, C., Qi, N.R., Burant, C.F., and Evans, C.R. (2015). Impact of anesthesia and euthanasia on metabolomics of mammalian tissues: studies in a C57BL/6J mouse model. PloS one *10*, e0117232.

Panda, S., Antoch, M.P., Miller, B.H., Su, A.I., Schook, A.B., Straume, M., Schultz, P.G., Kay, S.A., Takahashi, J.S., and Hogenesch, J.B. (2002). Coordinated transcription of key pathways in the mouse by the circadian clock. Cell *109*, 307-320.

Partch, C.L., Green, C.B., and Takahashi, J.S. (2014). Molecular architecture of the mammalian circadian clock. Trends Cell Biol *24*, 90-99.

Paschos, G.K., Ibrahim, S., Song, W.L., Kunieda, T., Grant, G., Reyes, T.M., Bradfield, C.A., Vaughan, C.H., Eiden, M., Masoodi, M., et al. (2012). Obesity in mice with adipocyte-specific deletion of clock component Arntl. Nat Med *18*, 1768-1777.

Pearce, S.F., Rorbach, J., Van Haute, L., D'Souza, A.R., Rebelo-Guiomar, P., Powell, C.A., Brierley, I., Firth, A.E., and Minczuk, M. (2017). Maturation of selected human mitochondrial tRNAs requires deadenylation. Elife *6*.

Peek CB, A.A., Ramsey KM, Kuo H, Yu W, Sena LA, Ilkayeva O, Marcheva B, Kobayashi Y, Omura C, Levine DC, Bacsik DJ, Gius D, Newgard CB, Goetzman E, Chandel NS, Denu JM, Mrksich M, Bass J (2013). Circadian Clock NAD+ Cycle Drives Mitochondrial Oxidative Metabolism in Mice. Science *342*, 8.

Piechota, J., Tomecki, R., Gewartowski, K., Szczesny, R., Dmochowska, A., Kudla, M., Dybczynska, L., Stepien, P.P., and Bartnik, E. (2006). Differential stability of mitochondrial mRNA in HeLa cells. Acta Biochim Pol *53*, 157-168.

Prut, L., and Belzung, C. (2003). The open field as a paradigm to measure the effects of drugs on anxiety-like behaviors: a review. Eur J Pharmacol *463*, 3-33.

Reddy, A.B., Karp, N.A., Maywood, E.S., Sage, E.A., Deery, M., O'Neill, J.S., Wong, G.K., Chesham, J., Odell, M., Lilley, K.S., et al. (2006). Circadian orchestration of the hepatic proteome. Curr Biol *16*, 1107-1115.

Robinson, B.G., Frim, D.M., Schwartz, W.J., and Majzoub, J.A. (1988). Vasopressin mRNA in the suprachiasmatic nuclei: daily regulation of polyadenylate tail length. Science *241*, 342-344.

Robles, M.S., Cox, J., and Mann, M. (2014). In-vivo quantitative proteomics reveals a key contribution of post-transcriptional mechanisms to the circadian regulation of liver metabolism. PLoS Genet *10*, e1004047.

Rorbach, J., and Minczuk, M. (2012). The post-transcriptional life of mammalian mitochondrial RNA. Biochem J *444*, 357-373.

Rorbach, J., Nicholls, T.J., and Minczuk, M. (2011). PDE12 removes mitochondrial RNA poly(A) tails and controls translation in human mitochondria. Nucleic Acids Res *39*, 7750-7763.

Rudic, R.D., McNamara, P., Curtis, A.M., Boston, R.C., Panda, S., Hogenesch, J.B., and Fitzgerald, G.A. (2004). BMAL1 and CLOCK, two essential components of the circadian clock, are involved in glucose homeostasis. PLoS Biol *2*, e377.

Saito, M., Okamatsu-Ogura, Y., Matsushita, M., Watanabe, K., Yoneshiro, T., Nio-Kobayashi, J., Iwanaga, T., Miyagawa, M., Kameya, T., Nakada, K., et al. (2009). High incidence of metabolically active brown adipose tissue in healthy adult humans: effects of cold exposure and adiposity. Diabetes *58*, 1526-1531.

Sendoel, A., Dunn, J.G., Rodriguez, E.H., Naik, S., Gomez, N.C., Hurwitz, B., Levorse, J., Dill, B.D., Schramek, D., Molina, H., et al. (2017). Translation from unconventional 5' start sites drives tumour initiation. Nature *541*, 494-499.

Shostak, A., Meyer-Kovac, J., and Oster, H. (2013). Circadian regulation of lipid mobilization in white adipose tissues. Diabetes *62*, 2195-2203.

Slomovic, S., Laufer, D., Geiger, D., and Schuster, G. (2005). Polyadenylation and degradation of human mitochondrial RNA: the prokaryotic past leaves its mark. Mol Cell Biol *25*, 6427-6435.

Storch, K.F., Lipan, O., Leykin, I., Viswanathan, N., Davis, F.C., Wong, W.H., and Weitz, C.J. (2002). Extensive and divergent circadian gene expression in liver and heart. Nature *417*, 78-83.

Stubblefield, J.J., Gao, P., Kilaru, G., Mukadam, B., Terrien, J., and Green, C.B. (2018). Temporal Control of Metabolic Amplitude by Nocturnin. Cell Rep *22*, 1225-1235.

Takahashi, J.S., Kumar, V., Nakashe, P., Koike, N., Huang, H.C., Green, C.B., and Kim, T.K. (2015). ChIP-seq and RNA-seq methods to study circadian control of transcription in mammals. Methods Enzymol *551*, 285-321.

Tomecki, R., Dmochowska, A., Gewartowski, K., Dziembowski, A., and Stepien, P.P. (2004). Identification of a novel human nuclear-encoded mitochondrial poly(A) polymerase. Nucleic Acids Res *32*, 6001-6014.

Turek, F.W., Joshu, C., Kohsaka, A., Lin, E., Ivanova, G., McDearmon, E., Laposky, A., Losee-Olson, S., Easton, A., Jensen, D.R., et al. (2005). Obesity and metabolic syndrome in circadian Clock mutant mice. Science *308*, 1043-1045.

Udagawa, T., Swanger, S.A., Takeuchi, K., Kim, J.H., Nalavadi, V., Shin, J., Lorenz, L.J., Zukin, R.S., Bassell, G.J., and Richter, J.D. (2012). Bidirectional control of mRNA translation and synaptic plasticity by the cytoplasmic polyadenylation complex. Mol Cell *47*, 253-266.

Ueda, H.R., Chen, W., Adachi, A., Wakamatsu, H., Hayashi, S., Takasugi, T., Nagano, M., Nakahama, K., Suzuki, Y., Sugano, S., et al. (2002). A transcription factor response element for gene expression during circadian night. Nature *418*, 534-539.

Vakifahmetoglu-Norberg, H., Ouchida, A.T., and Norberg, E. (2017). The role of mitochondria in metabolism and cell death. Biochem Biophys Res Commun *482*, 426-431.

van der Veen, D.R., Shao, J., Chapman, S., Leevy, W.M., and Duffield, G.E. (2012). A diurnal rhythm in glucose uptake in brown adipose tissue revealed by in vivo PET-FDG imaging. Obesity (Silver Spring) *20*, 1527-1529.

van Marken Lichtenbelt, W.D., Vanhommerig, J.W., Smulders, N.M., Drossaerts, J.M., Kemerink, G.J., Bouvy, N.D., Schrauwen, P., and Teule, G.J. (2009). Cold-activated brown adipose tissue in healthy men. N Engl J Med *360*, 1500-1508.

Virtanen, K.A. (2014). BAT thermogenesis: Linking shivering to exercise. Cell Metab *19*, 352-354.

Virtanen, K.A., Lidell, M.E., Orava, J., Heglind, M., Westergren, R., Niemi, T., Taittonen, M., Laine, J., Savisto, N.J., Enerback, S., et al. (2009). Functional brown adipose tissue in healthy adults. N Engl J Med *360*, 1518-1525.

Wang, X., Fang, H., Huang, Z., Shang, W., Hou, T., Cheng, A., and Cheng, H. (2013). Imaging ROS signaling in cells and animals. J Mol Med (Berl) *91*, 917-927.

Wang, Y., Osterbur, D.L., Megaw, P.L., Tosini, G., Fukuhara, C., Green, C.B., and Besharse, J.C. (2001). Rhythmic expression of Nocturnin mRNA in multiple tissues of the mouse. BMC developmental biology *1*, 9.

Waung, M.W., Pfeiffer, B.E., Nosyreva, E.D., Ronesi, J.A., and Huber, K.M. (2008). Rapid translation of Arc/Arg3.1 selectively mediates mGluR-dependent LTD through persistent increases in AMPAR endocytosis rate. Neuron *59*, 84-97.

Wehner, J.M., and Radcliffe, R.A. (2004). Cued and contextual fear conditioning in mice. Current protocols in neuroscience / editorial board, Jacqueline N. Crawley ... [et al.] *Chapter 8*, Unit 8 5C.

Weill, L., Belloc, E., Bava, F.A., and Mendez, R. (2012). Translational control by changes in poly(A) tail length: recycling mRNAs. Nat Struct Mol Biol *19*, 577-585.

Weinberg, J.M., Venkatachalam, M.A., Roeser, N.F., and Nissim, I. (2000). Mitochondrial dysfunction during hypoxia/reoxygenation and its correction by anaerobic metabolism of citric acid cycle intermediates. Proceedings of the National Academy of Sciences of the United States of America *97*, 2826-2831.

Wells, D.G., Dong, X., Quinlan, E.M., Huang, Y.S., Bear, M.F., Richter, J.D., and Fallon, J.R. (2001). A role for the cytoplasmic polyadenylation element in NMDA receptor-regulated mRNA translation in neurons. The Journal of neuroscience : the official journal of the Society for Neuroscience *21*, 9541-9548.

Woolum, J.C. (1991). A re-examination of the role of the nucleus in generating the circadian rhythm in Acetabularia. J Biol Rhythms *6*, 129-136.

Wydro, M., Bobrowicz, A., Temperley, R.J., Lightowlers, R.N., and Chrzanowska-Lightowlers, Z.M. (2010). Targeting of the cytosolic poly(A) binding protein PABPC1 to

mitochondria causes mitochondrial translation inhibition. Nucleic Acids Res *38*, 3732-3742.

Yamashita, A., Chang, T.C., Yamashita, Y., Zhu, W., Zhong, Z., Chen, C.Y., and Shyu, A.B. (2005). Concerted action of poly(A) nucleases and decapping enzyme in mammalian mRNA turnover. Nat Struct Mol Biol *12*, 1054-1063.

Yi, W., Clark, P.M., Mason, D.E., Keenan, M.C., Hill, C., Goddard, W.A., 3rd, Peters, E.C., Driggers, E.M., and Hsieh-Wilson, L.C. (2012). Phosphofructokinase 1 glycosylation regulates cell growth and metabolism. Science *337*, 975-980.

Zhang, R., Lahens, N.F., Ballance, H.I., Hughes, M.E., and Hogenesch, J.B. (2014). A circadian gene expression atlas in mammals: implications for biology and medicine. Proceedings of the National Academy of Sciences of the United States of America *111*, 16219-16224.

Zhang, X., Virtanen, A., and Kleiman, F.E. (2010). To polyadenylate or to deadenylate: that is the question. Cell Cycle *9*, 4437-4449.

Zvonic, S., Ptitsyn, A.A., Conrad, S.A., Scott, L.K., Floyd, Z.E., Kilroy, G., Wu, X., Goh, B.C., Mynatt, R.L., and Gimble, J.M. (2006). Characterization of peripheral circadian clocks in adipose tissues. Diabetes *55*, 962-970.